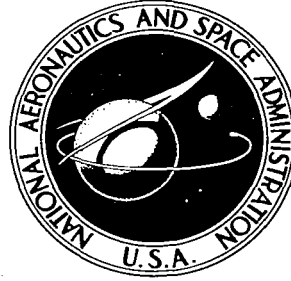


NASA TECHNICAL
REPORT



NASA TR R-198

C.1

NASA TR R-198

LOAN COPY: F
AFWL (W
KIRTLAND AF

0067987

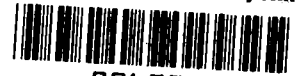


GROUND MEASUREMENTS OF
SONIC-BOOM PRESSURES FOR
THE ALTITUDE RANGE
OF 10,000 TO 75,000 FEET

*by Harvey H. Hubbard, Domenic J. Maglieri,
Vera Huckel, and David A. Hilton*

*Langley Research Center
Langley Station, Hampton, Va.*

TECH LIBRARY KAFB, NM



0067987

GROUND MEASUREMENTS OF SONIC-BOOM PRESSURES FOR
THE ALTITUDE RANGE OF 10,000 TO 75,000 FEET

By Harvey H. Hubbard, Domenic J. Maglieri,
Vera Huckel, and David A. Hilton

Langley Research Center
Langley Station, Hampton, Va.

NATIONAL AERONAUTICS AND SPACE ADMINISTRATION

For sale by the Office of Technical Services, Department of Commerce,
Washington, D. C. 20230 -- Price \$1.25

GROUND MEASUREMENTS OF SONIC-BOOM PRESSURES FOR
THE ALTITUDE RANGE OF 10,000 TO 75,000 FEET¹

By Harvey H. Hubbard, Domenic J. Maglieri,
Vera Huckel, and David A. Hilton
Langley Research Center

SUMMARY

Sonic-boom measurements are presented for flight tests of fighter and bomber airplanes in the altitude range from 10,000 to about 75,000 feet and at Mach numbers from 1.1 to 2 for a variety of atmospheric wind and temperature gradients and for various flight paths and acceleration rates. Measurements of the pressure signatures at 17 locations both parallel and perpendicular to the airplane flight track were recorded simultaneously and were synchronized in time.

The pressure signatures measured were similar to N-waves, but in all cases they differed in some detail. The shape of the pressure signature from a supersonic airplane is a function of atmospheric conditions, altitude, Mach number, flight path, configuration of the airplane, and relative position of the observer. Turbulent atmospheric conditions resulted in erratic wave shapes and in considerable variation in the measured peak overpressures for given flight conditions. As a result of airplane acceleration, more complex wave patterns and pressure magnifications are measured at some ground locations. The pressure magnification factors for a linear acceleration and a circular turn were noted to be approximately 2 and 4, respectively. The measured overpressures associated with very high-altitude, steady-flight conditions of the bomber airplane are noted to be greater than the predicted values.

INTRODUCTION

Because the sonic-boom problem may affect the design and operation of future supersonic transports (see refs. 1 and 2) and supersonic military aircraft, the U.S. Air Force, National Aeronautics and Space Administration, and Federal Aviation Agency have engaged in a joint research program to improve the level of technology with regard to this problem. Flight-test studies relating to the generation, propagation, and prediction of sonic booms have been conducted at Edwards Air Force Base, Calif., during September and October of 1961.

¹Supersedes NASA Technical Memorandum X-633 by Harvey H. Hubbard, Domenic J. Maglieri, Vera Huckel, and David A. Hilton, 1962.

The main objectives of these studies were to provide basic information relative to the generation of sonic booms in steady level flight at high altitudes where lift effects may be significant and relative to the phenomena of superbooms due to maneuvering flight. In addition, some experiments were performed to indicate the manner in which atmospheric phenomena affect sonic booms. The main variables of the tests were airplane configuration, weight, Mach number, altitude, flight path, and atmospheric wind and temperature gradients. Particular emphasis in the flight tests was placed on the use of instrumentation to record faithfully characteristic pressure signatures.

The purpose of this paper is to indicate the scope of the tests, to describe the special instrumentation and techniques used, and to discuss some of the results of preliminary analyses. A bibliography is also included for the convenience of the reader. A method for computing ground overpressures is presented in an appendix by Harry W. Carlson.

SYMBOLS

A	airplane cross-sectional area, sq ft
A(t)	nondimensionalized cross-sectional area A/l^2 at nondimensionalized station $t = x/l$
$A_E(t)$	effective nondimensionalized cross-sectional area due to a combination of volume and lift effects, $A(t) + B(t)$
B	equivalent cross-sectional area due to lift at airplane station x given by $B = \frac{\beta}{2q} \int_0^x F'_L dx$
B(t)	nondimensionalized equivalent cross-sectional area due to lift B/l^2 at nondimensionalized station $t = x/l$
C_L	lift coefficient
d	diameter of circle equivalent in area to the airplane cross-sectional area
F'_L	lifting force per unit length along airplane longitudinal axis
F(τ)	effective area distribution function, $\frac{1}{2\pi} \int_0^\tau \frac{A''_E(t)}{\sqrt{\tau - t}} dt$
h	airplane flight altitude

K_r	ground reflection factor
K_2	body shape factor
l	length of airplane, ft
M	Mach number
p	reference pressure, lb/sq ft
p_a	ambient pressure at altitude, lb/sq ft
p_0	ambient pressure at ground, lb/sq ft
Δp	incremental pressure above or below ambient pressure due to flow field of airplane, lb/sq ft
Δp_f	measured free-air pressure rise across shock wave, lb/sq ft
Δp_0	measured pressure rise across shock wave at ground level, lb/sq ft
Δp_r	measured reflected pressure rise across shock wave, lb/sq ft
q	dynamic pressure, lb/sq ft
S	wing planform area, sq ft
t	nondimensionalized distance along longitudinal axis from airplane
W	airplane weight, lb
x	distance measured along longitudinal axis from airplane or model nose
$\beta = \sqrt{M^2 - 1}$	
γ	ratio of specific heats for air, 1.4
τ	dummy variable of integration measured in same direction and with same units as t
τ_0	value of τ giving largest positive value of integral $\int_0^{\tau} F(\tau) d\tau$
μ	Mach angle, $\sin^{-1} \frac{1}{M}$

Subscript:

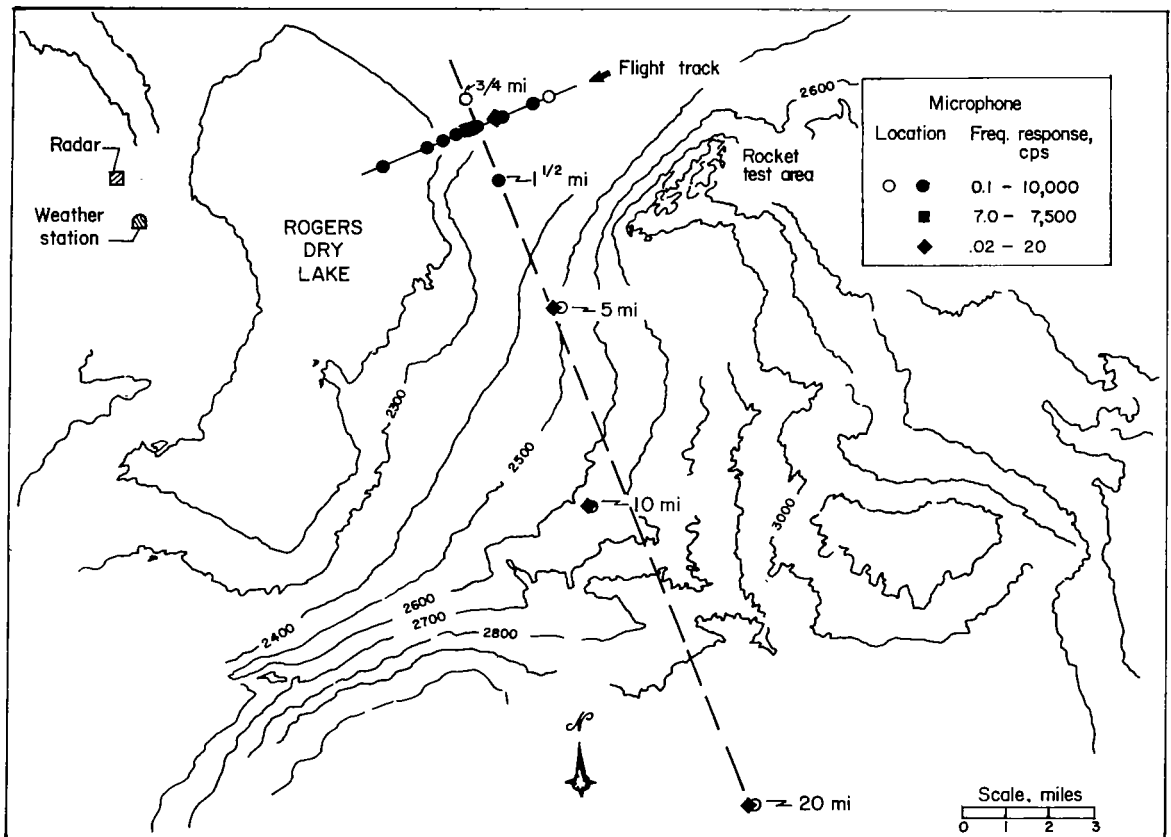
max maximum

A prime is used to indicate a first derivative, and a double prime, a second derivative with respect to distance.

APPARATUS AND METHODS

Test Conditions

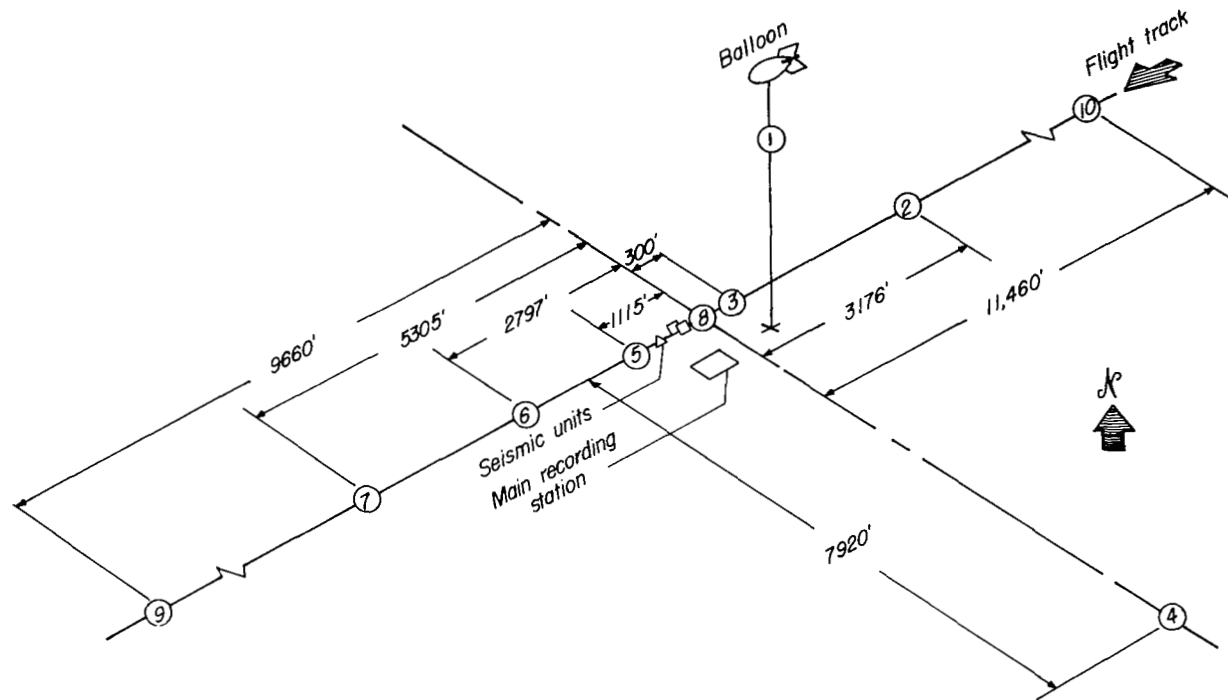
All test flights listed in table I were accomplished in the vicinity of the Edwards Air Force Base supersonic flight corridor and in the area just east of Rogers Dry Lake, Edwards, Calif. The terrain is generally flat with only sparse vegetation and has an altitude of 2,000 to 3,000 feet above sea level. As can be seen from figure 1(a), no extreme variations in elevation existed in the test area.



(a) General layout. Open symbols represent alternate microphone locations.

Figure 1.- Arrangement of test facilities and equipment.

The ground instrumentation was located in a T-shaped array, with 10 microphone locations in a line parallel to the center line of the supersonic flight corridor for a distance of about 4 miles. (See fig. 1(b).) This instrumentation was aligned along a heading of $245^{\circ}-065^{\circ}$ magnetic. Additional microphone



(b) Main station microphone arrangement. Numbers inside circles refer to specific microphones.

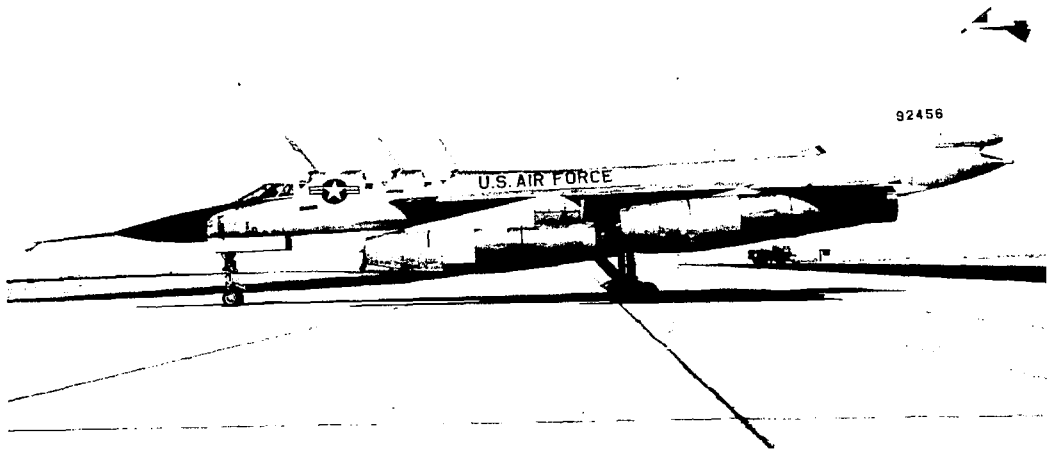
Figure 1.- Concluded.

stations (see fig. 1(a)) were located at lateral distances of about $\frac{3}{4}$, $1\frac{1}{2}$, 5, 10, and 20 miles and were aligned generally perpendicular to the arrangement parallel to the flight track. The main recording station was located near the intersection of the two instrument arrangements. (See fig. 1(b).) The accurate locations of all stations were established by means of standard surveying and optical techniques.

The tests were accomplished during September and October 1961. During this time the surface temperatures varied from about 50° to 95° and surface winds from 0 to about 35 statute miles per hour.

Test Airplanes

Photographs of the airplanes of the type used in these tests are shown in figure 2. The bomber airplane had an overall length of 96.8 feet and a gross



(a) Bomber.

L-61-8053



(b) Fighter.

Figure 2.- Photographs of airplanes of the type used in the flight tests. L-61-8054

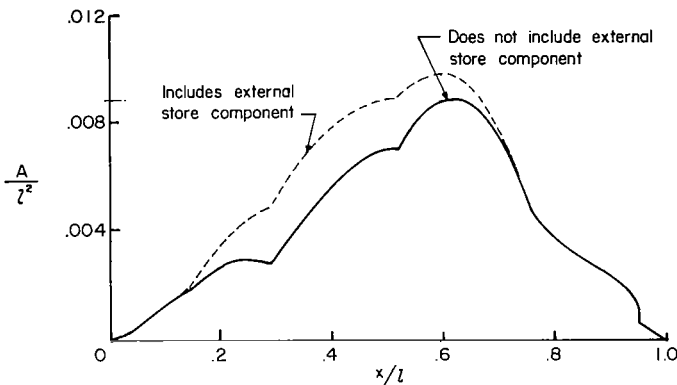
weight varying from about 63,000 to 90,000 pounds. The bomber airplane was operated in the configuration shown in figure 2(a) for all test flights. The airplane was operated without the detachable external store for the present tests, in contrast to those of reference 3 for which the external store was attached. The fighter airplane had an overall length of 54.5 feet, a gross weight of about 27,000 pounds, and was flown both with and without wing-tip tanks. The cross-sectional-area distributions for the bomber airplane both

with and without external store and for the fighter airplane without wing-tip tanks are given in figure 3. All test airplanes were provided, maintained, and operated by U.S. Air Force personnel.

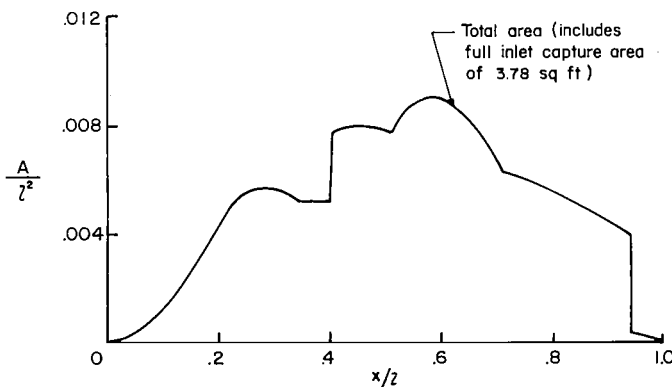
Airplane Positioning

The airplanes, in all cases, were positioned over the test area by means of ground-control procedures with the aid of radar tracking. For tests requiring steady-level-flight conditions, the pilot was provided corrections in heading by the ground controller only to within about 30 miles of the ground zero location of the main station. Changes in aircraft heading, speed, and altitude within the 30-mile distance were minimized in order to reduce possible effects on the sonic-boom ground-pressure patterns in the test area.

Radar plotting-board overlays were obtained for all flights, and the data obtained at 1-second intervals were used to provide information of the type shown in figure 4. For steady-flight conditions the data of the plotting-board overlay from which plan position, altitude, and speed can be obtained were of sufficient accuracy for purposes of the tests. For flights involving maneuvers, more accurate tracking data were obtained by the use of additional radar-tracking equipment and digital computing machine techniques.



(a) Bomber.



(b) Fighter.

Figure 3.- Area distribution of test aircraft.

altitude, and speed can be obtained were of sufficient accuracy for purposes of the tests. For flights involving maneuvers, more accurate tracking data were obtained by the use of additional radar-tracking equipment and digital computing machine techniques.

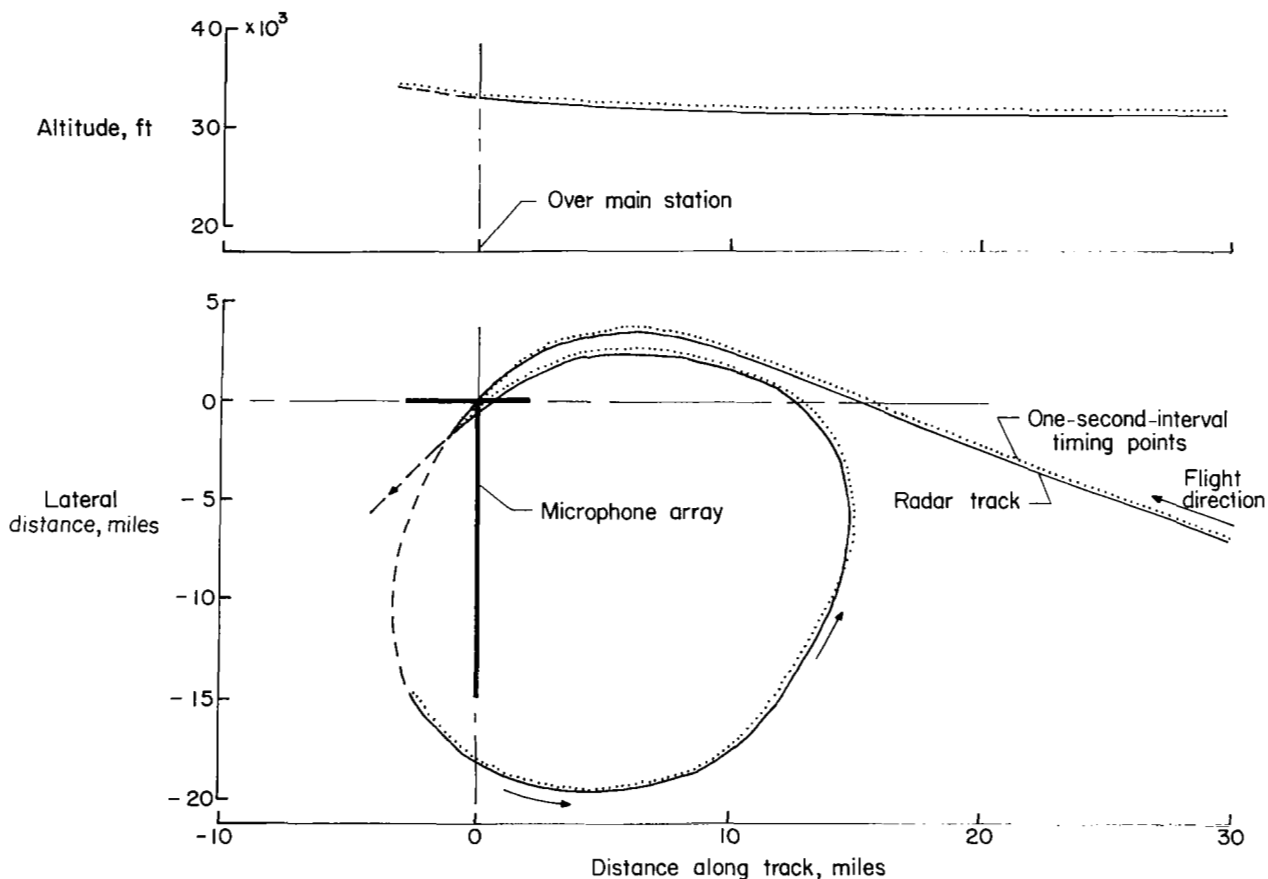


Figure 4.- Radar plotting-board track of airplane during circular-turn maneuver indicating both altitude and plan position as a function of distance along track. Data are for flight tests 32 and 33.

In order to synchronize the tracking data with all ground-pressure measurements, a 1,000-cps tone signal was superposed on the data records at the time the airplane passed over the main recording station.

Atmospheric Sounding

Rawinsonde observations from the Edwards Air Force Base weather facility, which was located within about 9 miles of the main recording station, were taken within 3 hours of the times of all test flights. Measured values of temperature and pressure, along with the calculated speed-of-sound and humidity values and wind-velocity and -direction values, were provided at 1,000-foot intervals to altitudes of about 5,000 feet in excess of the airplane test altitude. Samples of the atmospheric pressure, temperature, and speed-of-sound data for two of the test flights, along with the standard ICAO atmospheric values for comparison (ref. 4), are shown plotted as a function of altitude in

figure 5. Wind velocity has been resolved into components parallel to and perpendicular to the airplane flight path, and sample data are shown in figure 6.

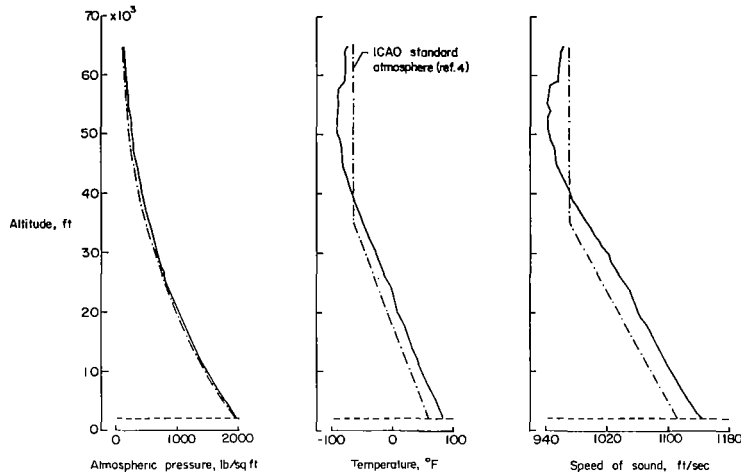
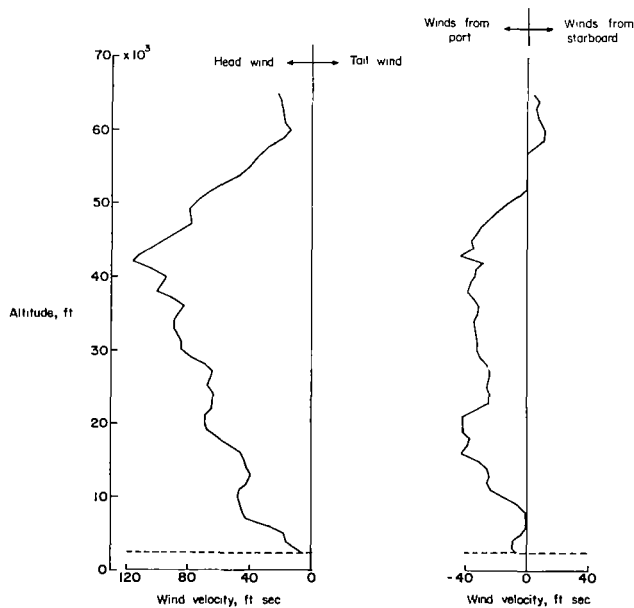


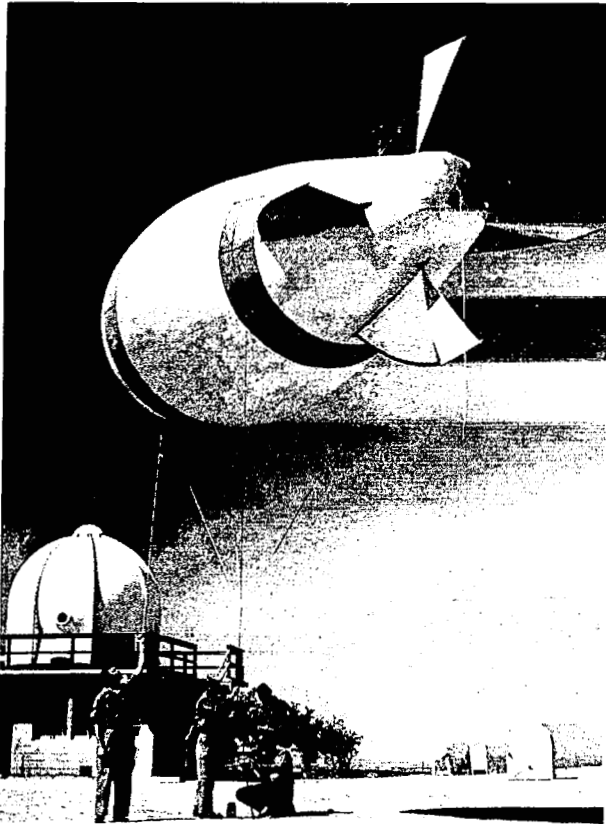
Figure 5.- Sample results from atmospheric soundings taken during test flights. Data are for flight tests 27 and 28.



(a) Component along flight path.

(b) Component perpendicular to flight path.

Figure 6.- Sample wind-velocity profiles resolved into components parallel to and perpendicular to the flight direction of the airplane. Data are for flight tests 27 and 28.



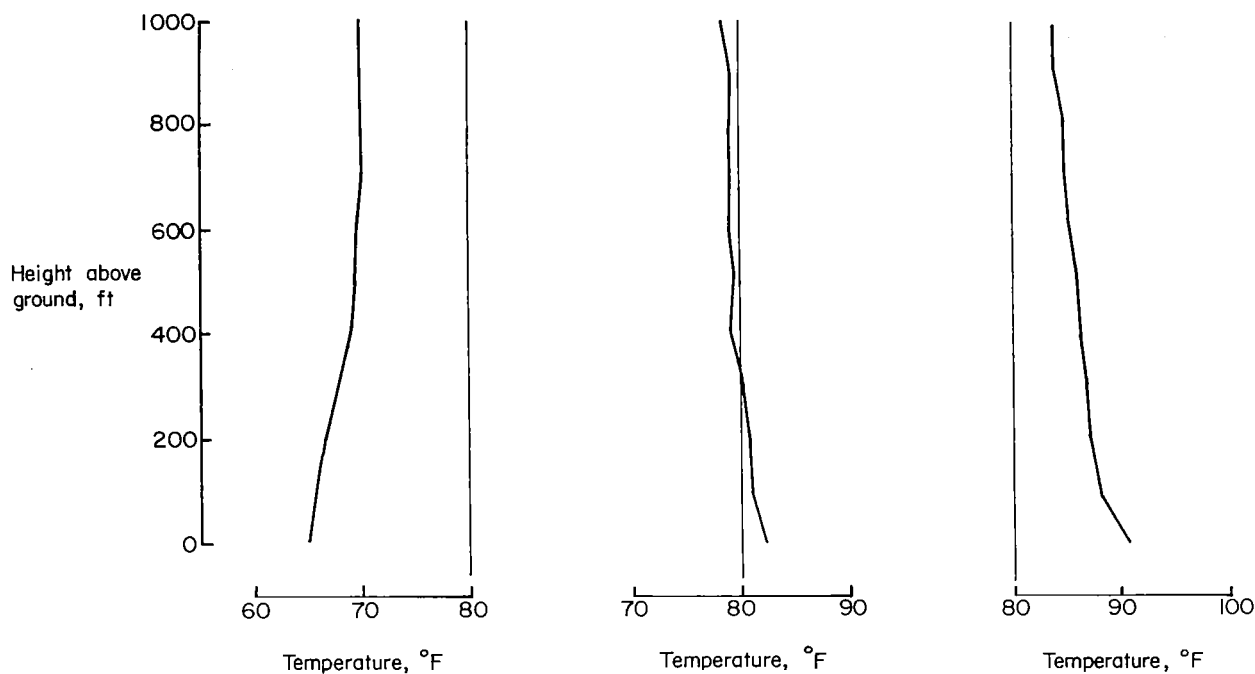
L-61-8055

Figure 7.- Photograph of wiresonde and auxiliary equipment used in obtaining atmospheric soundings at altitudes up to 1,000 feet.

Pressure, temperature, and relative humidity data were obtained with wiresonde equipment during the times of the tests at altitudes up to about 1,000 feet. The wiresonde equipment consists of a small instrument package which is connected by cable to monitoring instruments on the ground and which is positioned at various distances above ground level by means of a large, helium-filled balloon. The nature of this equipment is indicated in the photograph in figure 7. Data were obtained with the wiresonde equipment at intervals of 100 feet in altitude up to the maximum altitude of about 1,000 feet. Samples of the temperature data obtained are plotted in figure 8. Wiresonde information bridges the gap between surface measurements and those obtained during the rawinsonde soundings described previously. The type of information obtained from the wiresonde is useful in describing the conditions of the earth's boundary layer which, it is believed, may have significant effects on the sonic-boom signatures.

Ground-Pressure Instrumentation

The ground-pressure instrumentation provided and operated by the NASA consisted of an arrangement of special microphones located in an area measuring approximately 4 by 20 miles. The main recording station was located as shown in figure 1(b) and was arranged in such a manner that the signals from 11 of the microphones could be recorded simultaneously on magnetic tape. In addition to the main station arrangement, a satellite station with up to 2 microphone channels was mounted in a vehicle which could be positioned at various test locations within a 20-mile radius of the main station. Five measuring stations with microbarograph equipment were provided by the Atomic Energy Commission. One of these stations was located in the same area as the main microphone recording station, and the others were located at distances of about 5, 10, and 20 miles from the main station and in a direction generally perpendicular to the supersonic-flight corridor.



(a) September 14 at 0700 hours. (b) September 5 at 1200 hours. (c) September 5 at 1500 hours.

Figure 8.- Sample temperature-lapse rate data for three different atmospheric conditions encountered during the tests.

Three types of microphones were used. Commercially available condenser microphone measuring systems were specially modified in order to extend the frequency range from 10,000 cps on the high-frequency end to about 0.10 cps on the low-frequency end. The characteristics of this equipment were judged to be adequate to reproduce faithfully the sonic-boom signatures for the two airplanes and the various operating conditions of these tests. In addition to this special equipment, some commercially available condenser microphones of the type used in some previous sonic-boom investigations (refs. 3, 5, and 6) and with usable frequency responses in the range of about 7 cps to 7,500 cps were also used to provide comparative data. It is known that these microphones will not faithfully reproduce the sonic-boom signatures but will, however, provide true indications of the peak-pressure values. The third type of microphone used consisted of microbarograph equipment developed by the Atomic Energy Commission to have a flat frequency response in the range 0.02 to 20 cps. These microbarographs give a very good reproduction of the wave shapes except that they may not be able to follow the very rapid rise times of some of the waves and there may be some degradation of the peak-pressure values where very rapid rise times are involved because of the limited high-frequency response.

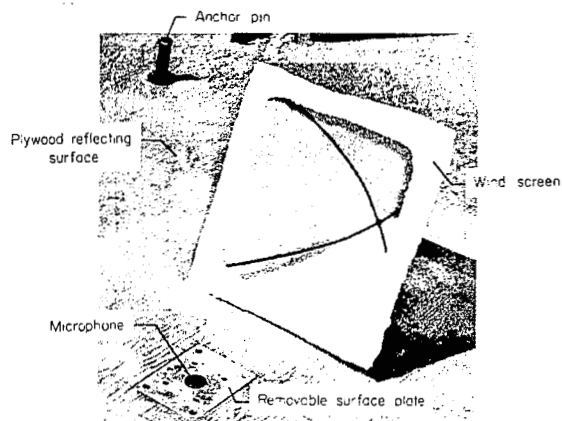
The commercially available microphone equipment was field calibrated acoustically with a 400-cycle signal applied at the microphone. The specially modified microphone equipment and the microbarograph equipment were field

calibrated statically before each test with the aid of a pressure bellows and a sensitive manometer. Prior to field installation, frequency-response curves were obtained for all microphones. Spot checks were also made over a range of frequencies during the field tests.

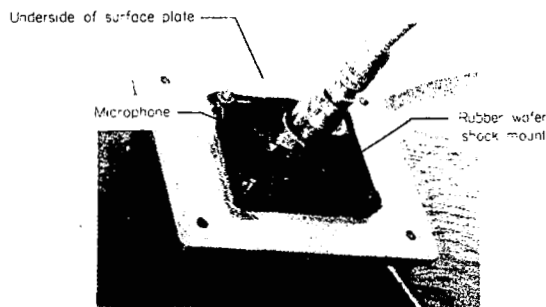
Special provisions were made to supply time synchronization for all pressure measurements. This synchronization was accomplished by transmitting a short burst of 1,000-cps tone from the radar station in such a manner that it was superposed on all pressure- and tracking-data records.

At the main recording station, pressure data were recorded simultaneously on magnetic tape for which the frequency response was flat from 0 to 20,000 cps and also on a conventional multichannel oscillograph for which the recording elements had a flat frequency response of 0 to 5,000 cps. All traces shown are from oscillograph recordings.

Most of the microphones were mounted at ground level to record the ground surface pressures. They were mounted in the surface of a 4- by 4-foot, 3/4-inch-thick plywood board staked down firmly to the ground. (See fig. 9(a).)



(a) Top view.



(b) Bottom view.

L-61-8056

Figure 9.- Details of ground microphone installation.

The microphone itself was suspended in a shock mount, as indicated in figure 9(b), at the center of the board to minimize spurious readings because of possible motions of the supports. Cheese-cloth screens, designed so that they would not affect the pressure measurements, were placed over the microphones to minimize the effects of wind on the microphone readings and also to provide shade from the sun and protection from blowing sand particles. Microphones were disassembled after each day's tests, and any accumulated dust was removed. In addition, a vertical arrangement of two microphones (one at ground level and one at a height of 30 feet directly above the other) was used to indicate the true shock-wave angle at ground level.

In order to provide additional information relative to the reflection of shock waves from the ground surface, special provision was made to elevate two of the pressure pickups during the tests. In one case a balloon which lifted a microphone to altitudes up to

approximately 290 feet above the ground station was used. In another case a 100-foot television tower was used for mounting a microbarograph. Free-air data were obtained both on the track of the airplane and at lateral distances up to 20 miles from the track.

Ground-Motion Instrumentation

A three-unit seismograph station was located in close proximity to the main pressure measuring station (see fig. 1(b)) and was oriented to measure the vertical and two horizontal components of ground motion. These units were attached to a metal plate set in a thin layer of concrete at the bottom of a 6-foot-deep hole in the ground and were subsequently buried under 5 to 6 feet of tamped earth. Simultaneous recordings of ground motion and pressure were made for correlation.

Check-Out of Pressure-Measuring Instrumentation

Past experience in the measurement of sonic-boom pressures during flight tests has indicated a substantial scatter in the results, as, for instance, in the work of reference 3. In order to separate out the normal instrument scatter from scatter because of possible atmospheric effects, a special flight test was conducted in the present investigation. The objective of this test was to obtain comparable data from several channels of measuring instrumentation of the same type under conditions where weather effects would be essentially eliminated. In order to do this, seven of the microphones having a frequency response of 0.10 to 10,000 cps were shock mounted in a reflection board within an area of less than 1 square foot. Data obtained from this instrument setup for a special flight test are illustrated in figure 10.

Data were obtained from a fighter airplane in steady flight at an altitude of 41,200 feet and at a Mach number of 1.52 (the quantity "altitude" is used consistently in the illustrations and tabulations of the present paper as the height of the aircraft above mean sea level). The test was accomplished at about 1400 hours at which time there was considerable atmospheric thermal activity in the test area.

The most obvious result of figure 10 is that the wave shapes show remarkable similarity. Although the peak amplitudes of the wave traces presented in figure 10 are not directly comparable because of variations in the sensitivity of the various channels of equipment, the measured peak values indicated in the figure are noted to be within a range of ± 15 percent or the equivalent of about ± 1 dB. Since it is believed that weather effects were essentially the same for each of these measurements, it is concluded that this amount of scatter may be ascribed to the instruments and measurement procedures and that scatter in excess of this amount in other tests would probably be due to other causes.

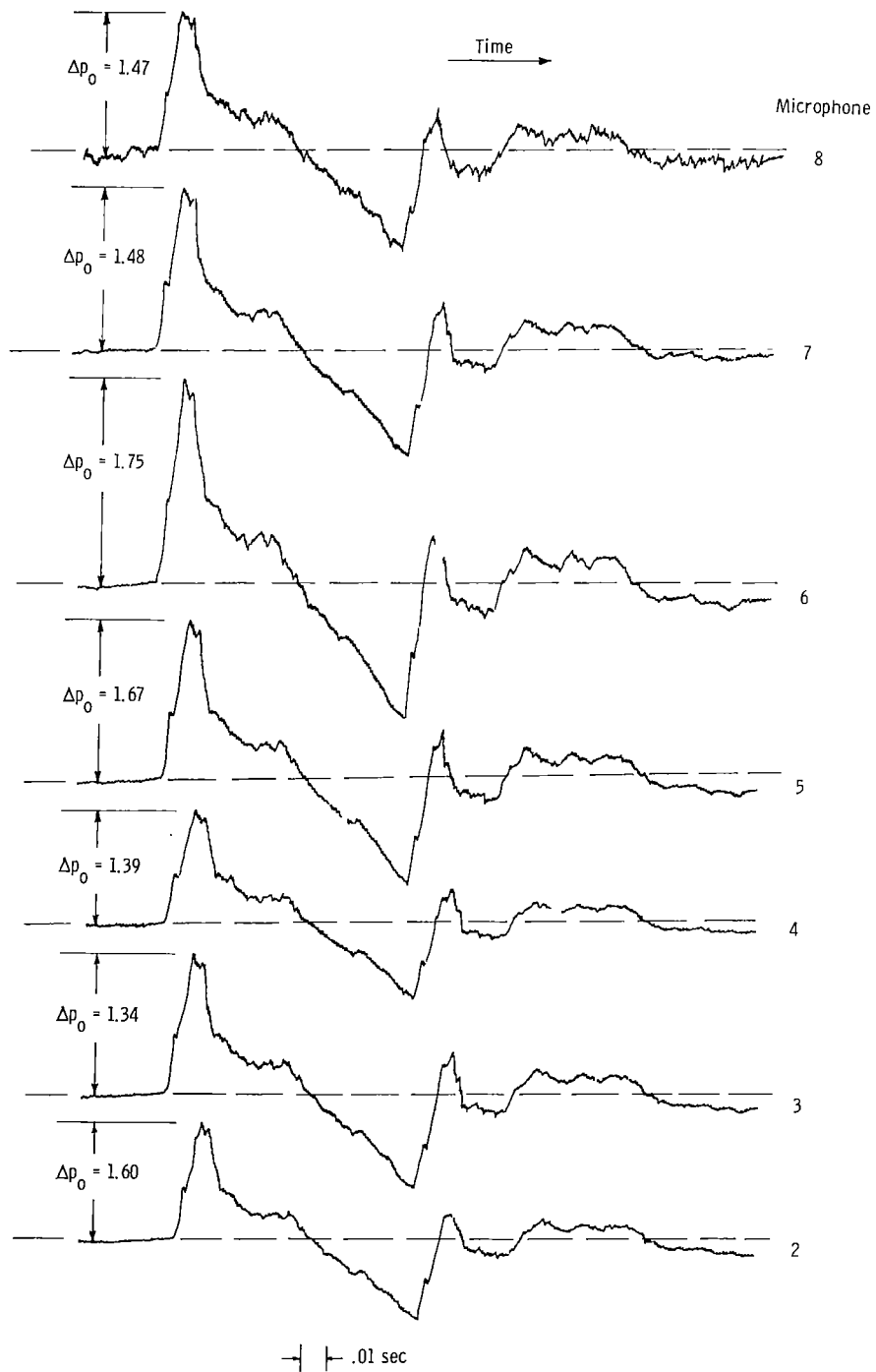


Figure 10.- Sonic-boom pressure signatures for a fighter airplane at an altitude of 41,200 feet and a Mach number of 1.52 from seven different microphones grouped within a 1-square-foot area on the ground. Data are from flight test 1. (Values of Δp_0 are expressed in pounds per square foot.)

DISCUSSION OF RESULTS

The data presented in this section of the paper have come from preliminary analyses of the test results. Not all data obtained during the flight tests are presented. Sample results of flight tests for fighter and bomber airplanes in steady flight at high altitudes and for fighter airplanes in maneuvers are presented. In addition to data which apply directly to these flight conditions, some indications of the effects of the atmosphere and reflections from the ground were obtained.

Effects of Various Parameters on the

Measured Pressure Signatures

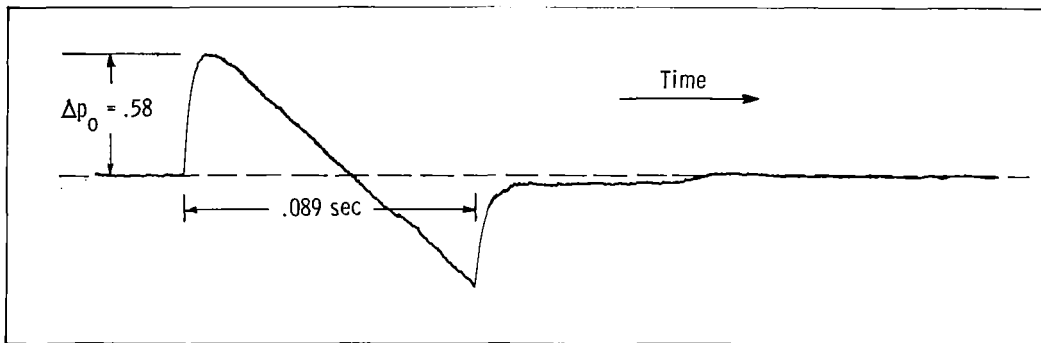
The atmosphere.- There was some concern for the results in figure 10 since the equipment used was adequate to have indicated an N-wave signature if one had existed. The reasons for deviation from the classical N-wave for the conditions in figure 10 were not known at the time, but subsequent tests suggested that these deviations were due to atmospheric effects. This phenomenon can be illustrated by the waveform data of figure 11.

The waveforms in figure 11 were obtained with the same measuring channel and for similar flight conditions but on different days and at different times of day. The airplane was in steady-level flight at a Mach number of about 1.92 and at an altitude of about 51,000 feet. The waveforms of figures 11(a), 11(b), and 11(c) were obtained in the morning and afternoon of one day and in the morning of another day, respectively.

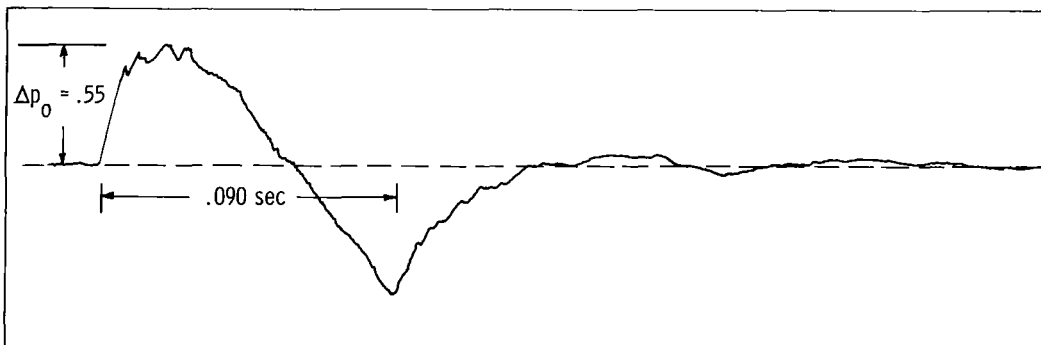
The waveform in figure 11(a) has the gross characteristics of the classical N-wave shape. It does, however, deviate from the N-wave shape in some important respects. The rate of onset of positive pressure is at first very rapid but then apparently falls off, with the result that the positive peak is rounded off. The slowly decreasing portion of the wave is essentially linear and terminates with a rapid recompression. The rate at which recompression occurs also apparently then reduces with the result that a rounding off back to atmospheric pressure occurs.

The waveform in figure 11(b) is significantly different than that for figure 11(a). For instance, the onset of positive pressure occurred at a much slower rate, the positive peak is broader as is the negative pressure peak, and the recompression to atmospheric pressure also occurs at a much slower rate. There are thus indications that small spurious pressure variations are superposed on the basic waveform.

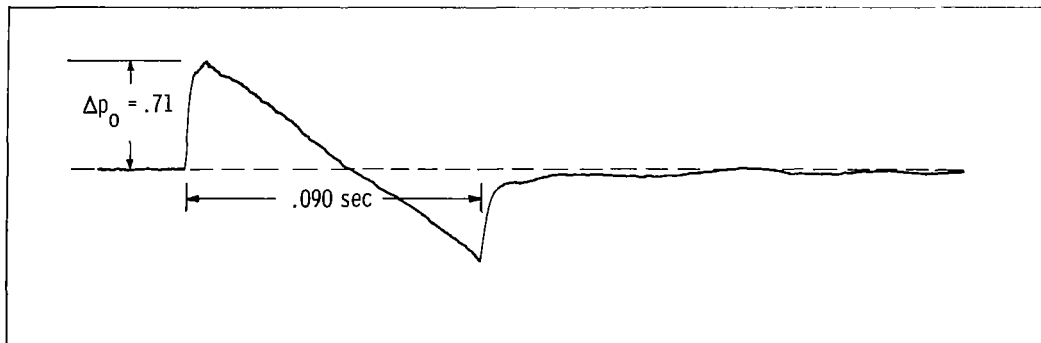
The waveform in figure 11(c) is very similar to that in figure 11(a). It is significant to note that the data in figures 11(a) and 11(c) were taken on different days but both were recorded during the early morning hours. The data in figure 11(b) were recorded during the afternoon. Atmospheric conditions, in particular those near the ground surface, were considerably different in the morning than in the afternoon in the area of the test site. During the morning



(a) Altitude, 53,100 feet; $M = 1.92$; 1000 hours.



(b) Altitude, 51,000 feet; $M = 1.92$; 1400 hours.



(c) Altitude, 51,000 feet; $M = 1.93$; 0940 hours.

Figure 11.- Tracings of sonic-boom ground-pressure signatures for three tests of a fighter airplane at steady-level-flight conditions but for different times of day. All three signatures were recorded with the same microphone system. Data are from flight tests 4, 5, and 6. (Values of Δp_0 are expressed in pounds per square foot.)

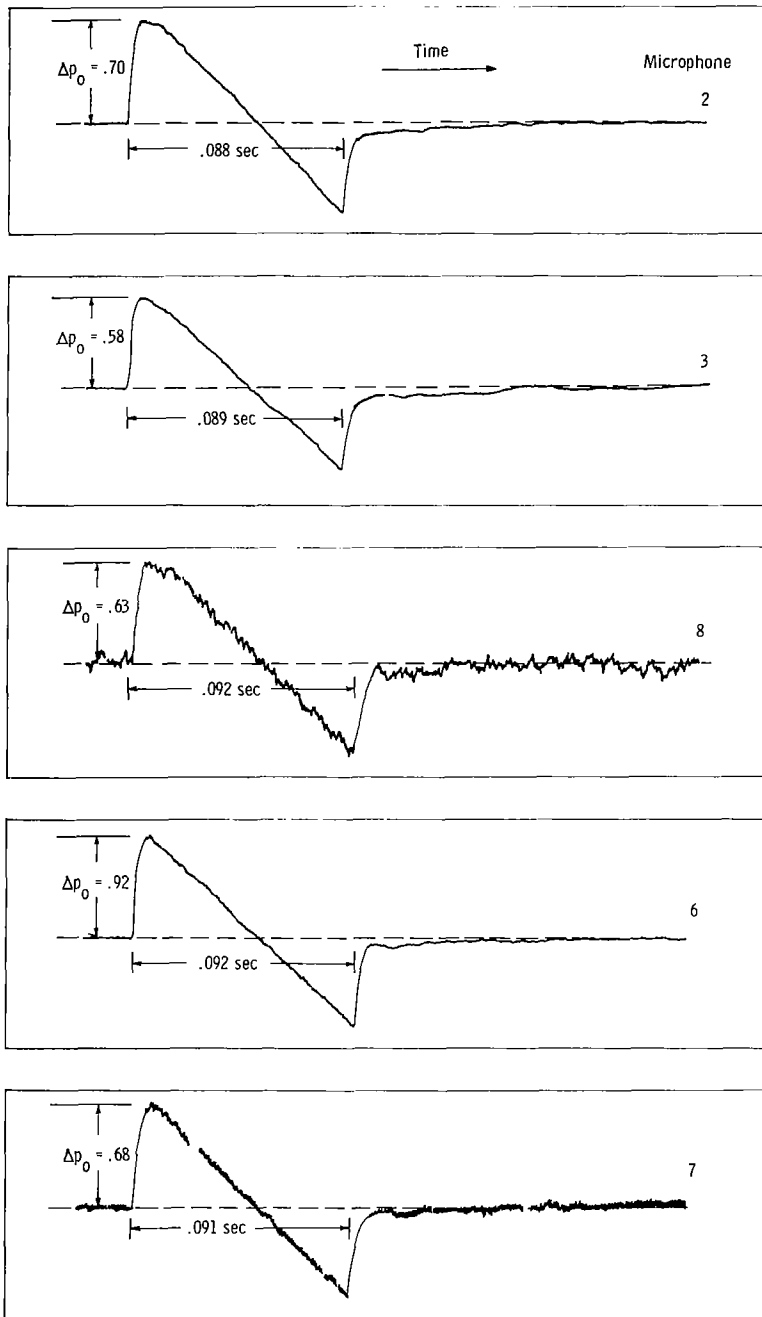
when a temperature inversion usually exists, as illustrated in figure 8(a), the atmosphere is quiescent. Later in the day as a superadiabatic temperature lapse-rate condition is reached, as illustrated in figure 8(c), the thermal activity increases and there is an increasing amount of atmospheric turbulence. There is, therefore, the suggestion that the waveforms recorded may be significantly affected by the convective activity in the atmosphere near the earth's surface.

This type of atmospheric effect would probably be somewhat different along each ray path; and therefore if measurements were made at a series of points along the ground track of the aircraft, the waveforms might be expected to differ from each other. In order to document these phenomena better, data from several microphones along the track are shown for the same flights as the data of figures 11(a) and 11(b) and are presented in figure 12. In figure 12(a) are presented the pressure signatures measured from 5 different microphones on the ground track of the aircraft which was flown at an altitude of about 53,100 feet and a Mach number of 1.92. The recordings were made at 1000 hours. It may be seen from the figure that the same general waveform existed at all measuring stations, and the pressure signatures differed from each other only in some small details. The high-frequency fluctuations on the records of microphones 7 and 8 are circuit noise from the power-supply units. As a matter of further information, the peak-pressure values were within ± 20 percent of the mean value.

In contrast to the results of figure 12(a), the pressure signatures of figure 12(b) are presented. These data are for approximately the same Mach number and altitude but were recorded at 1400 hours on the same day. It can be seen that the signatures at different measuring stations may be widely different in shape and in some cases bear only a slight resemblance to an N-wave. The rise times were noted to be generally longer than those of figure 12(a), and the peak-pressure values scattered as much as ± 50 percent from the mean value. It is believed that the main difference in the test conditions under which the two sets of data of figure 12 were obtained is the amount of convective activity in the atmosphere at the lower altitudes.

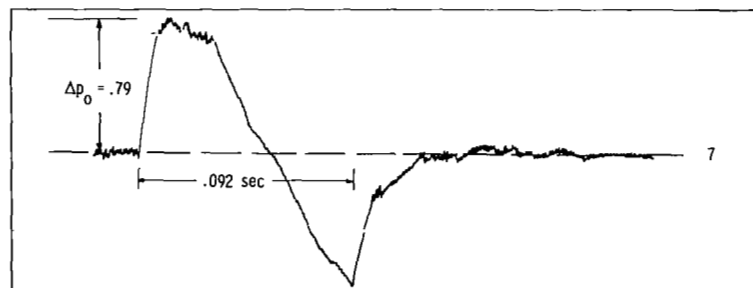
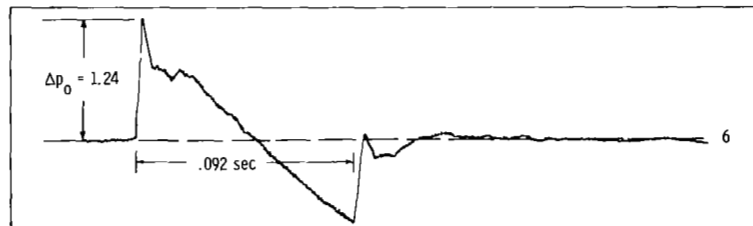
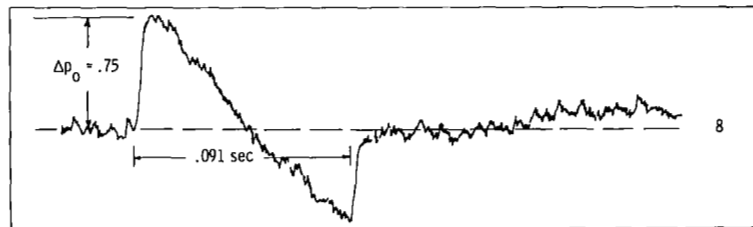
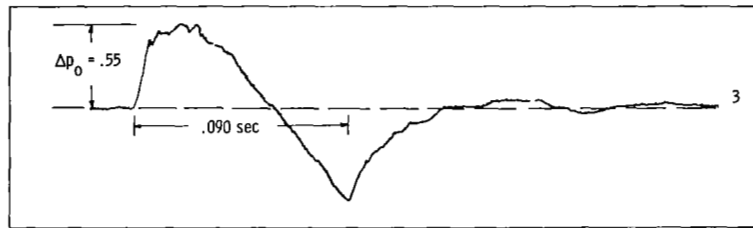
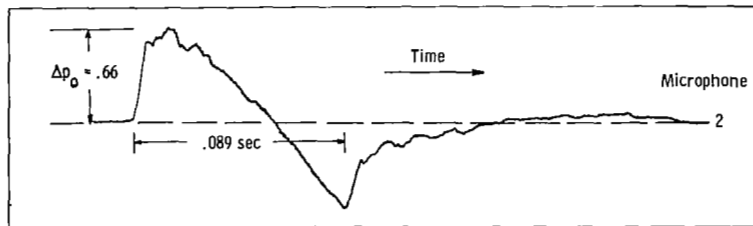
Aircraft configuration.- An additional way in which the pressure signatures may vary from the classical N-wave shape is illustrated in figure 13. It can be noted, for instance, in the tracing of figure 13(a) that an additional peak occurred in the record about midway between the first and last pressure rise. Based on previous experience, this additional pressure rise is probably associated with the geometry of the airplane, and in particular with the wing. (See ref. 7.) As the pressure field develops as a function of distance from the airplane, this disturbance tends to move forward as can be seen from the tracings of figure 13. For this particular airplane, coalescence with the bow wave apparently occurs at an altitude of about 50,000 feet. Although these trends seem to be mainly a function of altitude for this particular airplane, Mach number may also be significant for the range of Mach numbers covered.

Ground reflection.- The pressure signatures of figures 10 to 13 were measured at ground level and essentially consist of the incident and reflected waves added together in phase. Provision was also made to measure the incident (free air) and reflected components separately, and this was done with a microphone



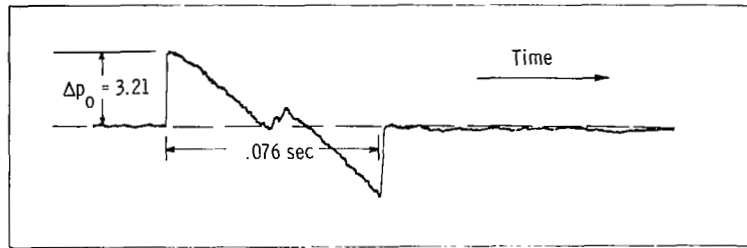
(a) Data recorded at 1000 hours (flight test 4).

Figure 12.- Sonic-boom ground-pressure signatures from five different microphones for the fighter airplane at a Mach number of 1.92 and an altitude of about 50,000 feet. (Values of Δp_0 are expressed in pounds per square foot.)

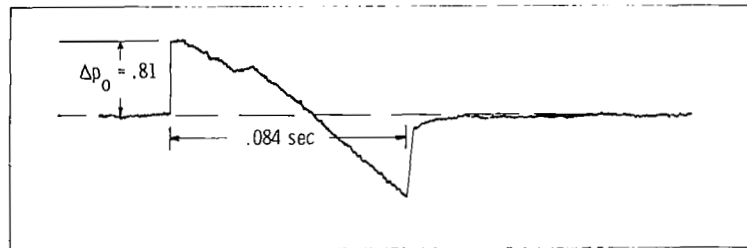


(b) Data recorded at 1400 hours (flight test 5).

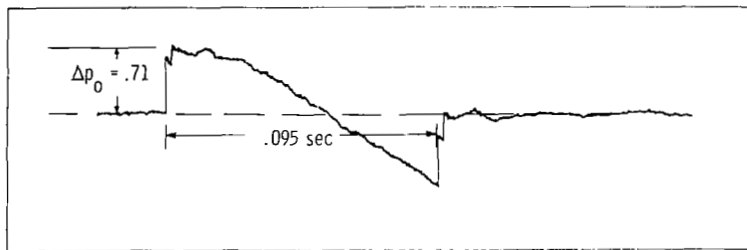
Figure 12.- Concluded.



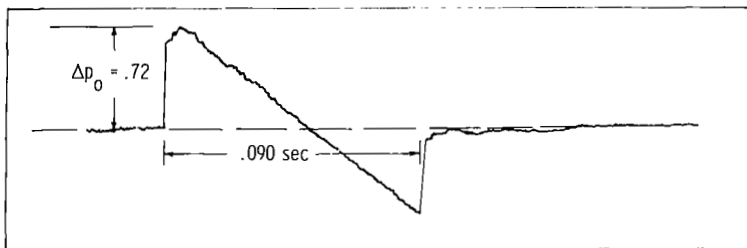
(a) Test 14; altitude, 10,300 feet; $M = 1.24$.



(b) Test 25; altitude, 32,200 feet; $M = 1.34$.



(c) Test 22; altitude, 43,200 feet; $M = 1.44$.



(d) Test 6; altitude, 51,000 feet; $M = 1.93$.

Figure 13.- Tracings of sonic-boom ground-pressure signatures from the fighter airplane at various altitudes and Mach numbers. (Values of Δp_0 are expressed in pounds per square foot.)

suspended above the ground surface by means of a balloon. Some sample results of such experiments for both fighter and bomber airplanes are given in figure 14.

The type of signature obtained is a function of the height of the measuring point above ground, the Mach number of the airplane, and the spacing of the waves which in turn is a function of the airplane configuration and its altitude. The tracings of figures 14(a) and 14(c) are for the fighter and bomber airplanes, respectively, and the test conditions were such that the incident and the reflected waves are separated. It can be seen that the gross features of the two components in each case are similar and that the peak pressures are approximately equal. (The reflecting surface in each case was the hard flat dry lake bed.)

A somewhat different result is illustrated in figure 14(b) in which the test conditions were such that the incident and reflected components were not separated. For the case illustrated, the reflected wave is superposed on the incident wave but is not in phase with it. For a given airplane and for given flight conditions, various phasing combinations would exist depending on the height of the observation point above the ground reflecting surface.

Curved flight path.- More than a single N-wave may also be observed as a result of curved flight of an airplane (ref. 8). In such a maneuver the ray paths may converge with the result that pressure buildups occur in some areas on the ground in excess of those which result from steady flight at comparable conditions. Such pressure buildups are referred to as "superbooms" and are believed to occur when disturbances from more than one point on the airplane flight path arrive at a point on the ground at nearly the same time. It is, of course, possible for disturbances from more than one point along the flight path of the airplane to reach the same point on the ground at different times during a turning maneuver of the airplane. Data illustrating this latter phenomenon are presented in figure 15.

The data of figure 15 apply to a circular turn maneuver of the type illustrated in the plan-position radar track of figure 4 and were recorded at a position on the ground near the main recording station. The airplane was at an altitude of 32,200 feet, a Mach number of 1.43, and was operated in a 1.5g circular turn. In addition to the conventional N-wave pressure signature, a tracing of which is shown at the top of figure 15, a second and a third waveform were also recorded subsequently at time intervals of 0.92 and 1.17 seconds, respectively, after the first waveform. The waveforms which arrived at the later times were noted to have longer time periods and lower peak pressures. These three waveforms are believed to have propagated in such a manner as to arrive at the same measuring station on the ground at the time intervals indicated. At other measuring stations on the ground, similar results were obtained except that the time intervals between waveforms differed.

For other flight conditions and for a similar turn maneuver, measurements were made of a superboom in which the peak pressures were about four times those anticipated for steady-level flight at the same conditions. It is believed that in this latter case waveforms from more than one location on the flight path

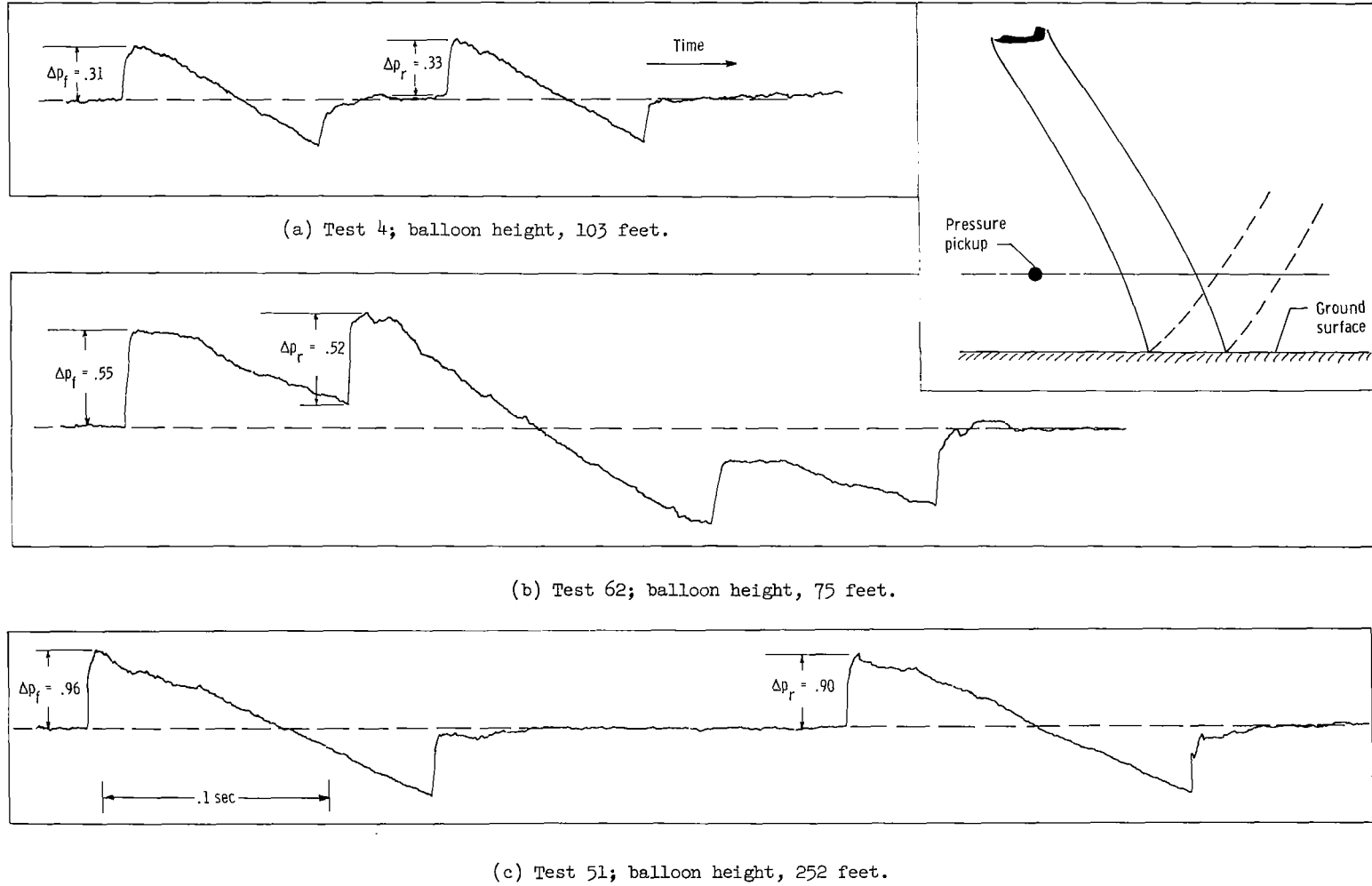
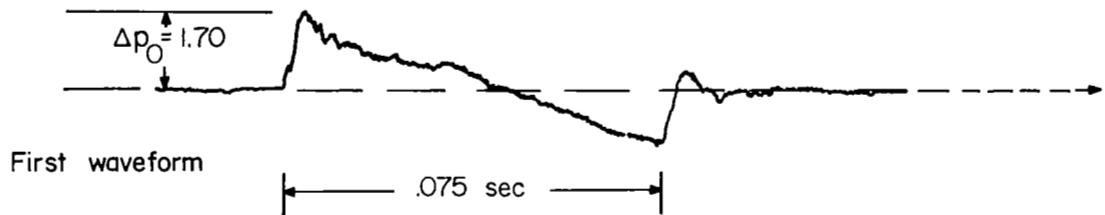
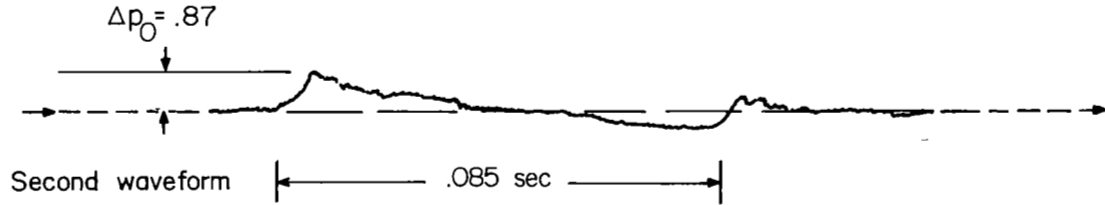


Figure 14.- Tracings of free-air and reflected sonic-boom pressure signatures obtained with the aid of a microphone suspended from a balloon at various distances above the ground. (Values of Δp_f and Δp_r are expressed in pounds per square foot.)



Time interval between first and second waveform, 0.92 sec



Time interval between second and third waveform, 0.25 sec

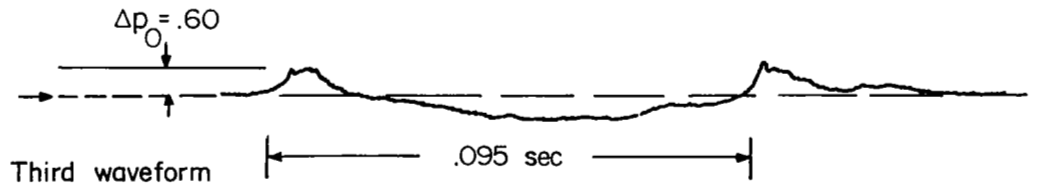


Figure 15.- Tracings of sonic-boom ground-pressure waveforms recorded at a location near the flight track during the circular-turn maneuver of the type shown in figure 4. Data are from flight test 18. (Values of Δp_0 are expressed in pounds per square foot.)

probably arrived at the given ground measuring station at the same time. The manner in which such a phenomenon might take place is illustrated by the waveform tracings of figure 16.

Airplane linear acceleration.- Data are presented for four different measuring stations along the ground track of the fighter airplane during linear acceleration at low supersonic speeds. At measuring stations 2, 3, 6, and 7 as identified in figure 1(b), it can be seen that two types of N-wave pressure waveforms were measured. The first of these was, in each case, the stronger of the two and had the shorter time period. Furthermore, it can be seen that the time interval between the first and second waveforms changes progressively from a relatively large value at station 7 to a rather small value at station 3. Measurements at intermediate locations, which are not included in the figure, were consistent with those shown. At station 2 it is believed that this progression has continued to the point where the two waves are nearly superposed. When this happens, the peak pressure is noted to be approximately twice that measured at any of the other measuring stations. The orderly progression of waves illustrated in figure 16 is believed to be illustrative of the manner in which superbooms occur.

Airplane altitude.- Ground-pressure signatures have been obtained for the bomber airplanes for a range of altitudes from about 30,000 to 75,000 feet and for a range of Mach numbers from about 1.5 to 2.0. Representative tracings of some of these waveforms obtained on the ground track at the same microphone location for several different flights are presented in figure 17. It can be seen that all the waveforms presented are of the N-wave type and are similar in nature to those that have been presented for the fighter airplanes. They do, however, differ in that the peak pressures are somewhat higher and the time intervals are longer for comparable flight conditions.

In general, it can be seen that the peak-pressure values decrease and the time intervals increase as the altitude of the bomber aircraft is increased. It may also be seen that the return to atmospheric pressure at the end of the pressure signature is accomplished in a shorter time for the bomber airplane of figure 17 than for the fighter airplane of figure 12. In all cases there is a very sudden onset of positive pressure followed by a rounding off of the positive peak, as was previously noted for the fighter airplane. There are no distinct additional peaks present between the two main pressure peaks as were noted for the fighter airplanes in figure 13. There is, however, a suggestion of the presence of some additional mild disturbances for altitudes below about 50,000 feet. An additional general result is that the positive impulse, as represented by the area under the positive part of the curve, is consistently greater than the negative impulse for the bomber airplane as well as for the fighter airplane. The significance of this asymmetry is not fully understood at this time although it is believed that the effects of lift would at least partly account for it.

Airplane lateral distance.- Ground-pressure signatures have been obtained at various lateral distances up to 20 miles from the ground track for the bomber airplane at an altitude of about 61,000 feet and at a Mach number of about 2.0. Tracings of some of these measured signatures are presented in figure 18. Also

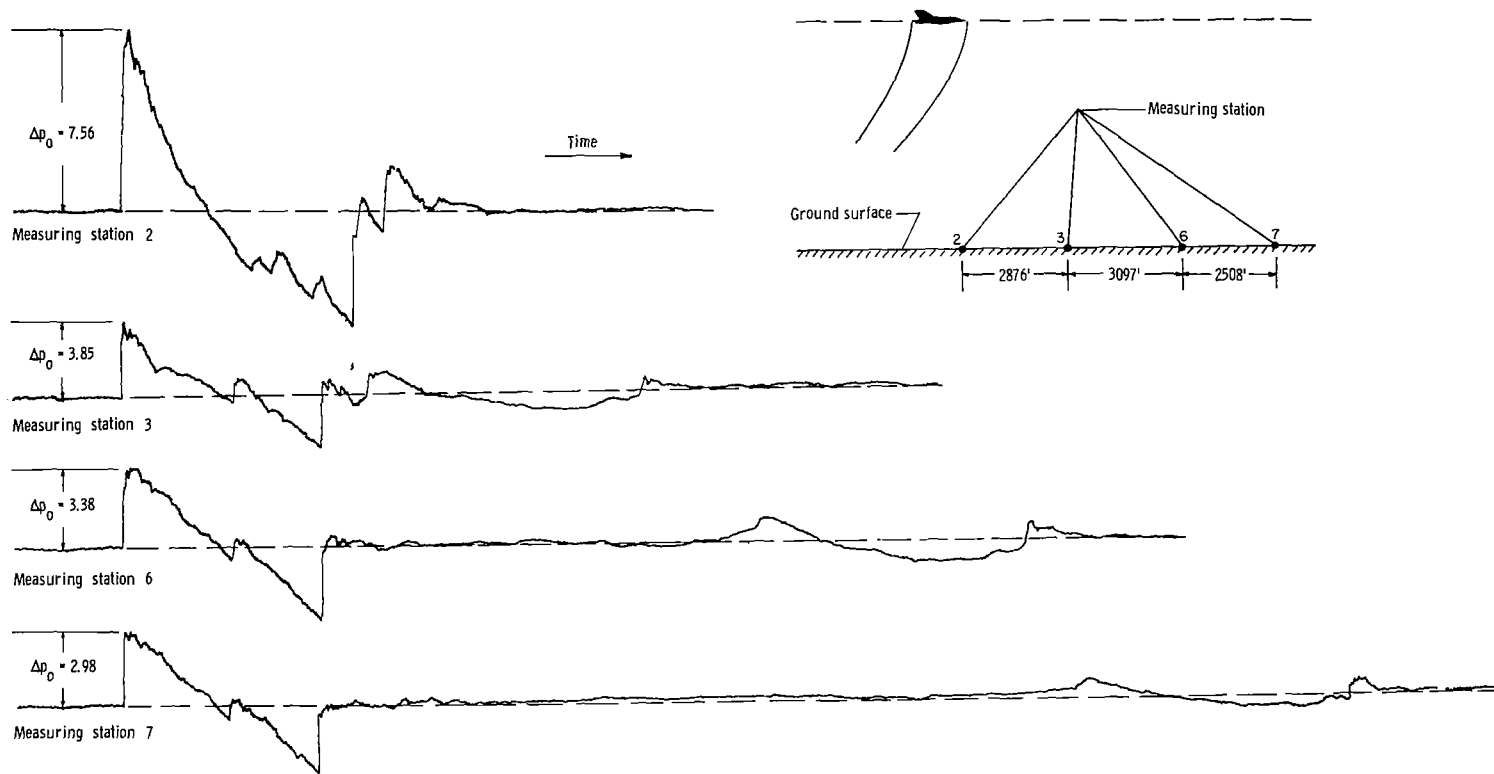
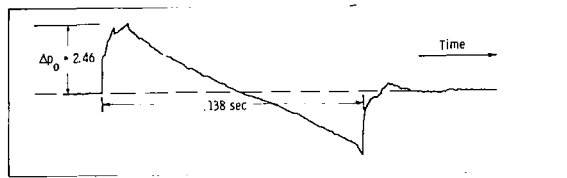
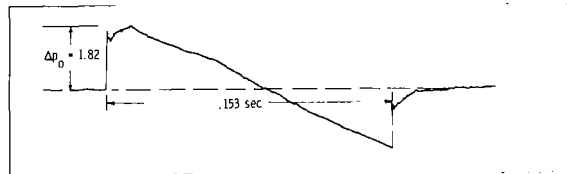


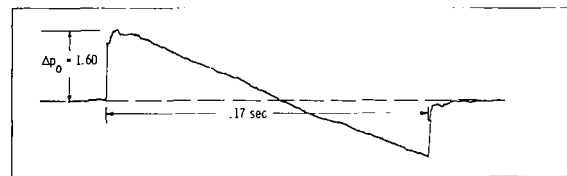
Figure 16.- Tracings of sonic-boom pressure waveforms measured at four stations along the flight track during linear acceleration of the fighter airplane at an altitude of 14,200 feet. Data are from flight test 20. (Values of Δp_0 are expressed in pounds per square foot.)



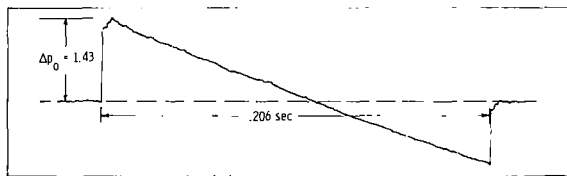
(a) Altitude, 31,200 feet; M = 1.5.



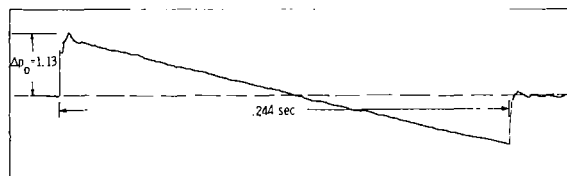
(b) Altitude, 42,100 feet; M = 1.8.



(c) Altitude, 51,600 feet; M = 2.0.

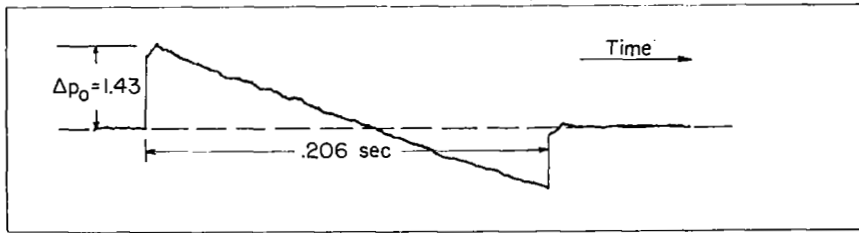


(d) Altitude, 61,100 feet; M = 2.0.

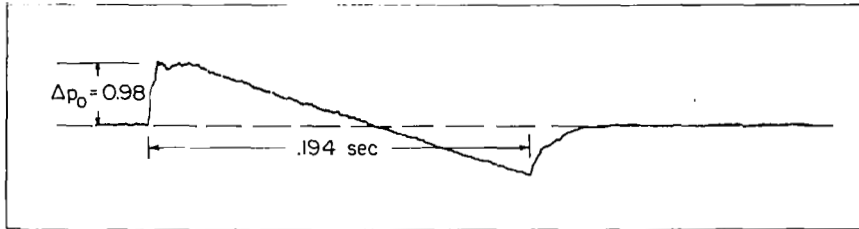


(e) Altitude, 70,700 feet; M = 1.72.

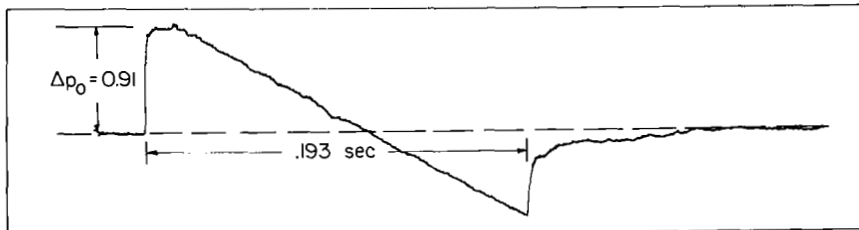
Figure 17.- Tracings of sonic-boom ground-pressure signatures for the bomber airplane at various altitudes and Mach numbers. (Values of Δp_0 are expressed in pounds per square foot.)



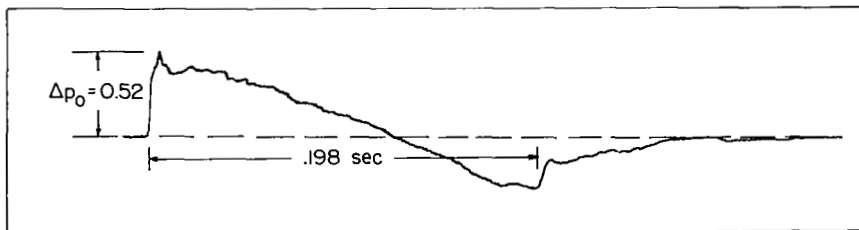
(a) On ground track.



(b) 5-mile lateral distance.



(c) 10-mile lateral distance.



(d) 20-mile lateral distance.

Figure 18.- Tracings of sonic-boom ground-pressure signatures at various lateral distances from the ground track for the bomber airplane at an altitude of about 61,000 feet and a Mach number of 2.0. (Values of Δp_0 are expressed in pounds per square foot.)

presented in the figure are peak overpressures and time-interval values measured for each test. Here again, as in figure 17, the pressure signatures are seen to have the gross features of N-waves. At the larger lateral distances, however, they seem to have a more ragged appearance, possibly a result of atmospheric effects in propagation. A notable difference is that at the lateral-distance locations there is a relatively slow rise time and a relatively slow return to atmospheric pressure as compared with the data of figure 17 which were obtained on the ground track. In general, the peak-pressure values decrease gradually as the lateral distance increases. The time intervals, however, do not seem to vary in a systematic manner with increasing distance as was the case for increasing altitude in figure 17.

Peak Overpressure Measurements

Peak overpressures have been determined from pressure-signature records similar to those of figures 10 to 18 for the flight tests of the fighter and bomber airplanes, and these values are plotted in figures 19 to 21. The fighter-airplane data of figure 19 are for the altitude range of about 10,000 to 50,000 feet and apply directly to locations on the ground track. Values of

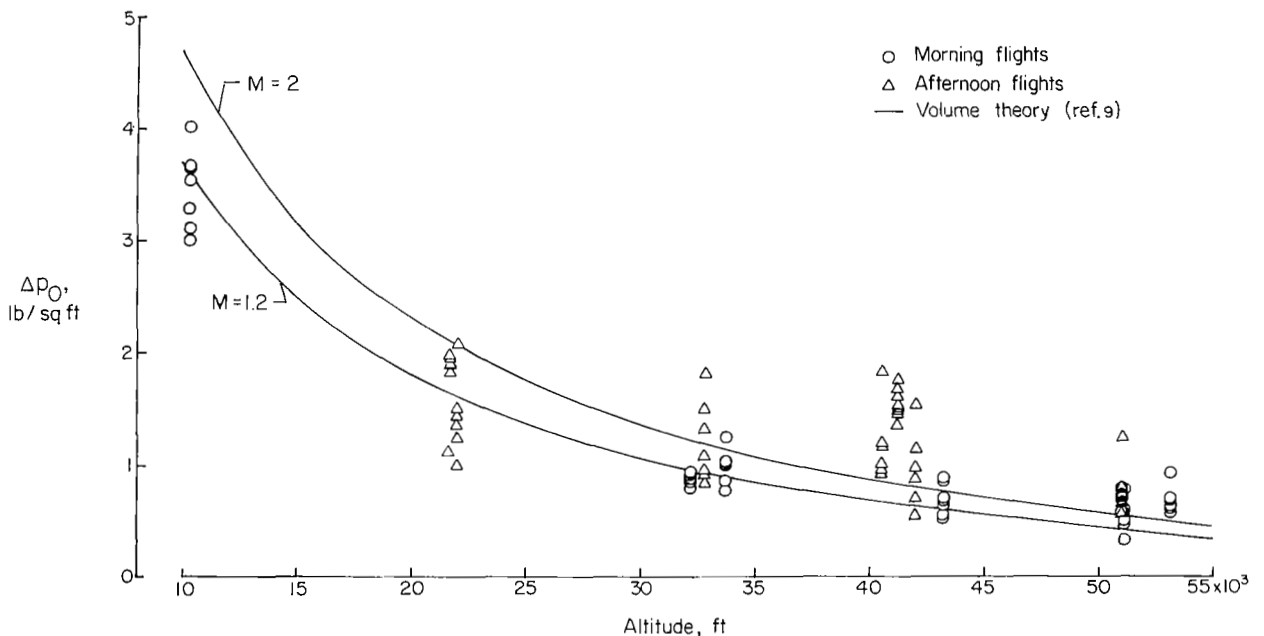


Figure 19.- Measured peak overpressures at ground level as a function of altitude for fighter airplanes in steady level flight. Data are included for both morning and afternoon flights.

Δp_0 vary from about 4 pounds per square foot to about 0.4 pound per square foot. Data points are coded to indicate that some apply to conditions of a quiescent atmosphere as in figure 12(a) and that some apply to conditions of a turbulent atmosphere as in figure 12(b). The two calculated curves are

for Mach numbers of 1.2 and 2.0 and are based on volume considerations only, a standard atmosphere being assumed, by means of the following equation from reference 9:

$$\Delta p_0 = K_r \frac{\sqrt{p_a p_0}}{h^{3/4}} (M^2 - 1)^{1/8} K_2 \left(\frac{d}{l}\right) (l)^{3/4} \quad (1)$$

For the calculations of figure 19,

$$K_r = 1.9$$

$$K_2 = 0.60$$

$$l = 54.5 \text{ feet}$$

$$d/l = 0.12$$

In general, the measured points scatter about the calculated curves, the highest values and the greatest scatter being associated with turbulent atmospheric conditions.

The peak ground overpressures determined for the bomber aircraft are presented as a function of altitude for an altitude range 30,000 to 75,000 feet and for a Mach number range of 1.5 to 2.0 in figure 20. The data points are coded to indicate the various gross-weight ranges of the aircraft during a rather extensive series of flight tests without the external store component and for a limited number of flights with the external store component. Also included for comparison are theoretical calculations based on a standard atmosphere for volume only and for volume and lift combined. The solid curve was calculated by means of equation (1) and for the following values:

$$K_r = 1.9$$

$$K_2 = 0.62$$

$$l = 96.8 \text{ feet}$$

$$d/l = 0.12$$

The cross-hatched region represents the range of ground overpressure values (which were calculated by means of eq. (A1) and have been evaluated by the numerical method described in the appendix and also in ref. 10). This procedure represents an attempt to account for both volume and lift effects for the gross-weight range of 62,000 to 92,000 pounds.

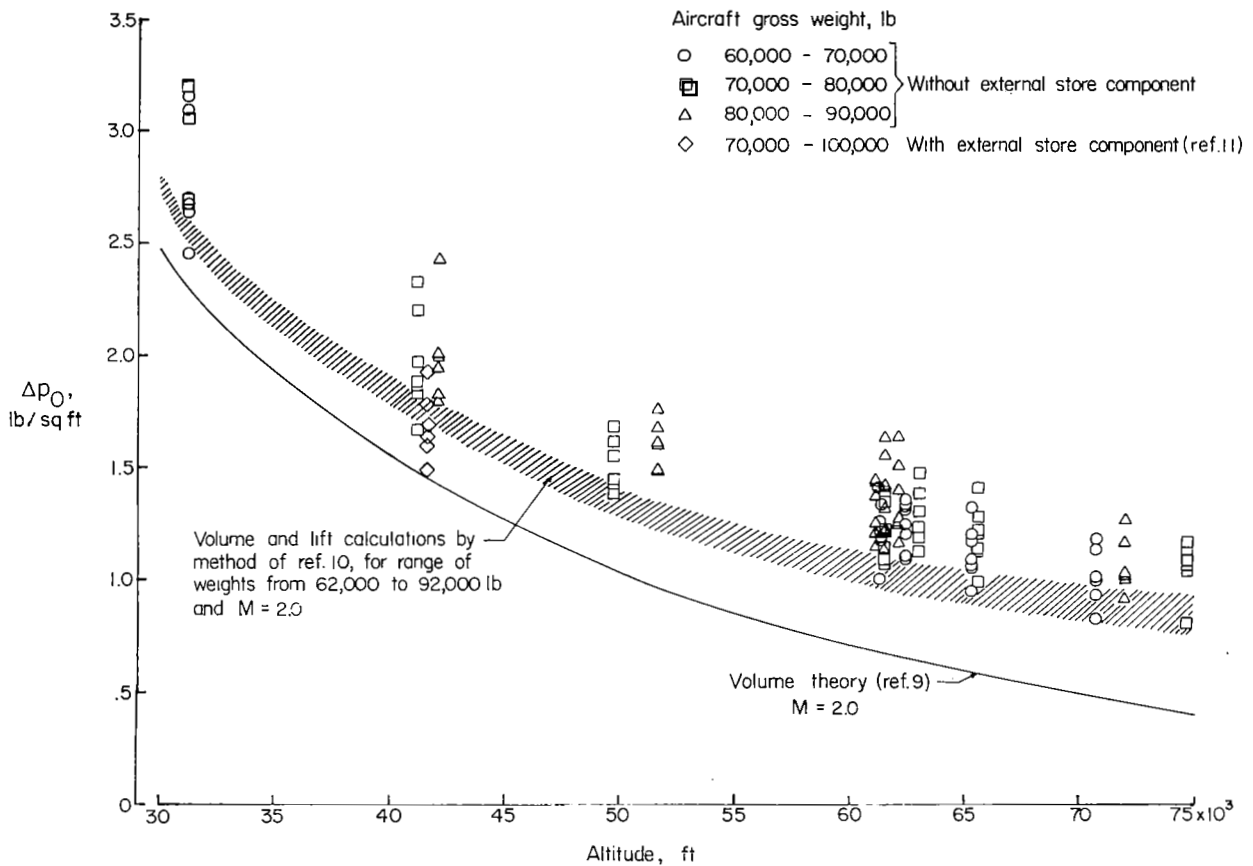


Figure 20.- Measured peak overpressures at ground level as a function of altitude for bomber airplanes in steady level flight. Data are presented for a range of Mach numbers from 1.5 to 2.0.

The experimental data of figure 20 are seen to have some scatter which is partly due to the gross-weight variations of the tests and partly to measuring techniques and atmospheric effects. In general, the measured overpressure values decrease as the altitude increases, those pressures associated with the higher gross weights having the higher values. It may be seen that the measured data clearly fall above the calculated curve based on volume effects only; thus, lift effects are suggested to be significant for the whole range of altitudes of these flight tests and particularly for the higher altitudes. It may be seen further that the experimental data fall generally above the calculations where lift and volume have both been taken into account, the one exception being the series of recent data points obtained during flights with the external store component. (See ref. 11.) These latter data are noted to be lower in magnitude than comparable values obtained without the external store in place. This latter finding is in qualitative agreement with similar wind-tunnel and analytical studies of reference 12.

Peak ground overpressures measured during the tests for various lateral distances up to 20 miles from the flight track and for flight conditions of a Mach number of 2.0 and an altitude range of 61,000 to 66,000 feet are presented in figure 21. These data points were determined from pressure waveforms of the

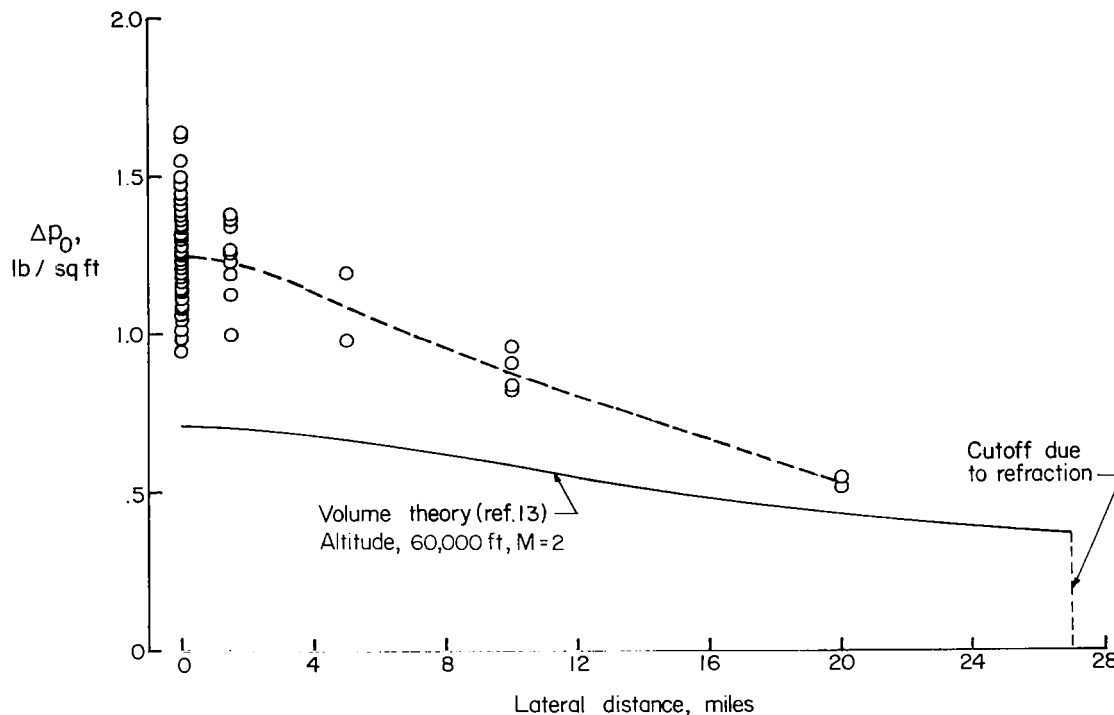


Figure 21.- Measured peak overpressures at ground level as a function of lateral distance for bomber airplanes in steady level flight. Data are for the altitude range of 61,000 to 66,000 feet and for a Mach number of about 2.0.

type presented in figure 18. The solid curve was calculated based on volume considerations alone by the method of reference 13, for which a cutoff distance of 27 miles due to refraction is indicated. The dashed curve is faired through the arithmetic average value of the measured pressures at each location. The measured values decrease as lateral distance increases; as a result, at a distance of 20 miles from the flight track the pressure values are approximately one-half those measured on the ground track. The measured values are consistently higher than the calculated values shown, although these differences are noted to be greater at locations near the track. This result suggests that the effects of lift may be most significant at locations on the track and at the smaller lateral distances.

Ground-Motion Measurements

For all the flights listed in table I, measurements of ground motion were made in a vertical plane as well as parallel and perpendicular to the direction of flight in a horizontal plane. Although some motions were recorded in each of the three directions for each flight test, the peak amplitudes did not exceed 0.001 inch. The largest motions were noted to occur in the vertical plane and in the horizontal plane parallel to the direction of flight. The records indicated a damped sine-wave type of motion having a frequency of about 10 cps, and it is believed that the disturbances were of a localized nature.

CONCLUDING REMARKS

The pressure signatures measured were similar to N-waves, but in all cases they differed in some detail. The shape of the pressure signature from a supersonic airplane is noted to be a function of atmospheric conditions, altitude, Mach number, flight path, configuration of the airplane, and relative position of the observer. As a result of changes in flight path or acceleration of the airplane, a more complex wave pattern is measured for maneuvering flight than for steady level flight, and for some ground locations pressure magnifications occur. The magnification factors for a linear acceleration and a circular turn were noted to be approximately 2 and 4, respectively. Effects of lift are noted to be significant for the bomber airplane for altitudes from 30,000 to about 75,000 feet and are more pronounced at the higher altitudes. Lift effects as detected by ground-pressure measurements are more pronounced directly under the aircraft and tend to decrease at increased lateral distances.

Langley Research Center,
National Aeronautics and Space Administration,
Langley Station, Hampton, Va., February 5, 1964.

APPENDIX

METHOD FOR COMPUTING GROUND OVERPRESSURES

By Harry W. Carlson

Outline of Method

An outline of the theoretical method used in estimating the intensity of the far-field bow-shock pressure rise directly below an airplane in level supersonic flight is shown in figure 22. The method shown here is in a form suitable for a numerical solution with desk calculators or with electronic computing

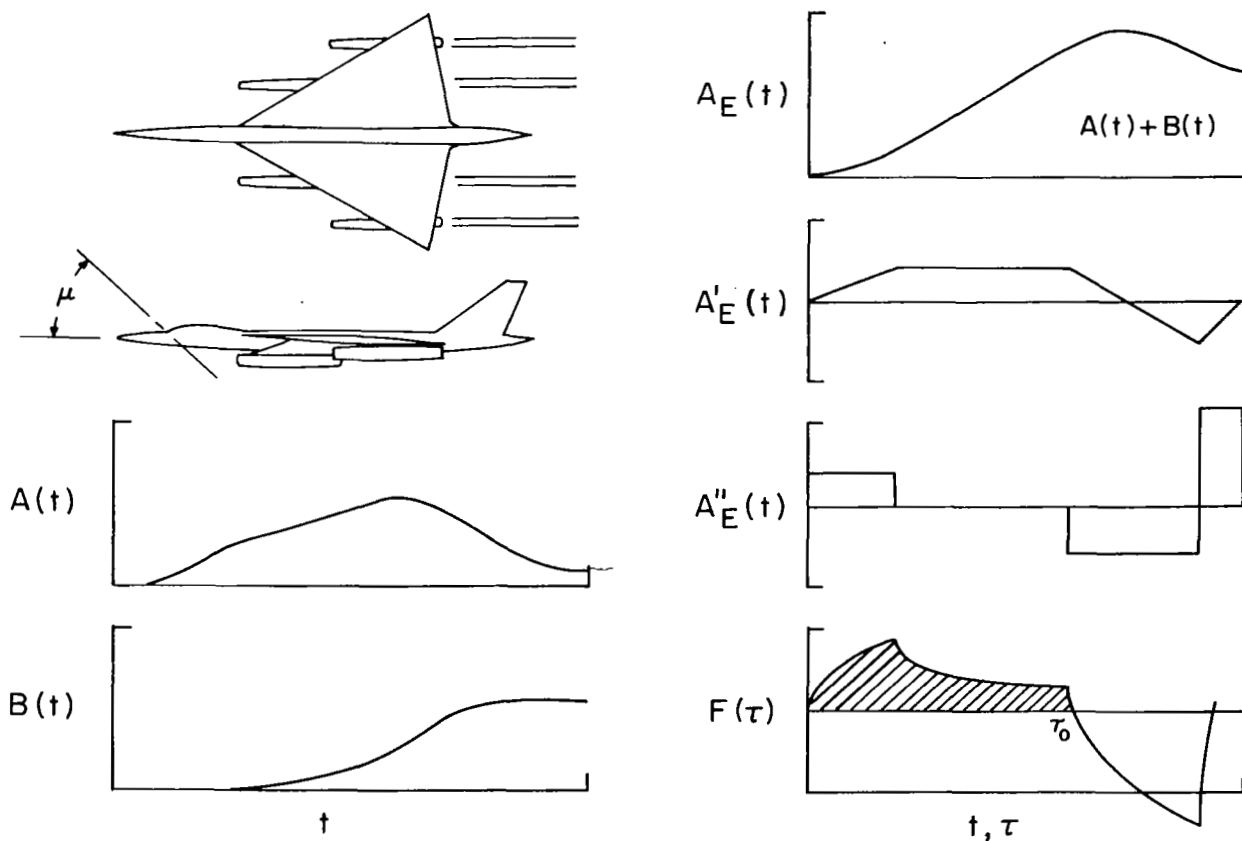


Figure 22.- Outline of steps in theoretical estimation method.

machines. It has been derived from the work of reference 14; the main differences stem from changes in terminology and in the expression of lift effects in terms of equivalent cross-sectional area. The following equation relates overpressure to the geometry of the airplane and the flight conditions.

$$\frac{\left(\frac{\Delta p}{p}\right)_{\max} \left(\frac{h}{l}\right)^{3/4}}{K_r \beta^{1/4}} = \frac{1.19\gamma}{\sqrt{\gamma + 1}} \sqrt{\int_0^{\tau_0} F(\tau) d\tau} \quad (A1)$$

The right-hand side of the equation depends only on the lift distribution and the geometry of the airplane and is evaluated in the following manner. The necessary inputs to the computation are a nondimensionalized airplane area distribution $A(t)$ formed by supersonic area rule cutting planes ($\mu = \sin^{-1} \frac{1}{M}$) and a nondimensionalized equivalent area distribution due to lift $B(t)$ evaluated through an integration of the lifting force per unit length along the airplane longitudinal axis. The $B(t)$ curve which is evaluated from the integral

$$B(t) = \frac{\beta}{2ql^2} \int_0^x F'_L dx \quad (A2)$$

is seen to depend on the weight of the airplane, the Mach number, and the dynamic pressure, in addition to the shape of the loading curve. A combined area distribution $A_E(t)$ is formed by a direct addition of the $A(t)$ and $B(t)$ curves. The $A_E(t)$ curve is then approximated by a series of parabolic arcs having a first derivative composed of connected straight-line segments and a second derivative composed of a step or pulse function. The integral involved in the $F(\tau)$ function

$$F(\tau) = \frac{1}{2\pi} \int_0^{\tau} \frac{A''_E(t)}{\sqrt{\tau - t}} dt$$

can be evaluated easily when $A''_E(t)$ is a constant, and by superposition a complete $F(\tau)$ curve may be built up corresponding to the $A''_E(t)$ pulse distribution. An integration of the $F(\tau)$ function to the point τ_0 (cross-hatched area in fig. 22) is then used in evaluating the pressure-rise characteristics expressed by equation (A1). The degree of approximation of the $A_E(t)$ curve can be improved by increasing the number of pulses used. In the machine computing procedure used for the estimates of this report the airplane length is divided into 100 units.

Results Obtained by Method

When the preceding computational procedures are followed for a series of assumed weights, Mach numbers, and dynamic pressures, the results are

conveniently expressed in the form shown in figure 23. As a matter of interest, theoretical curves are shown for the cases where volume effects alone or lift

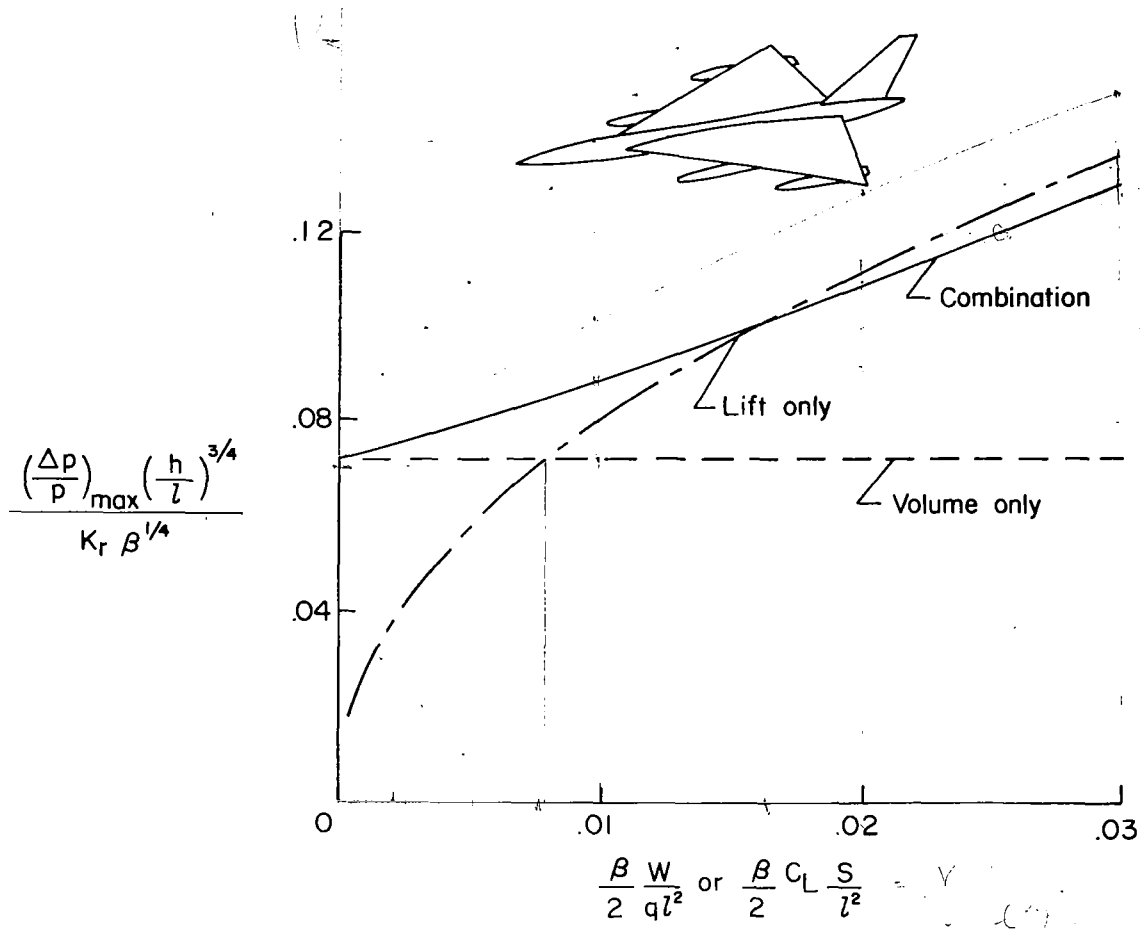


Figure 23.- Configuration sonic-boom characteristics in parametric form.

effects alone were considered. The results may be considered to apply for a range of Mach numbers, if changes in area and lift distribution with Mach number are ignored. Estimates of ground overpressures may be made when proper values of the factors in the parameters are substituted. For the estimates of this report, the reflection factor was assumed to be 2.0 and the reference pressure p was taken as the geometric mean of the pressure at altitude and the pressure at ground level $\sqrt{p_a p_0}$.

REFERENCES

1. Nichols, Mark R.: *The Supersonic Transport - Required Characteristics of Configurations*. [Preprint] 341F, Soc. Automotive Eng., 1961.
2. Hubbard, Harvey H., and Maglieri, Domenic J.: *Noise Considerations in the Design and Operation of the Supersonic Transport*. *Noise Control Shock and Vibration*, vol. 7, no. 4, July-Aug. 1961, pp. 4-10.
3. Maglieri, Domenic J., and Hubbard, Harvey H.: *Ground Measurements of the Shock-Wave Noise From Supersonic Bomber Airplanes in the Altitude Range From 30,000 to 50,000 Feet*. NASA TN D-880, 1961.
4. Minzner, R. A., Ripley, W. S., and Condron, T. P.: *U.S. Extension to the ICAO Standard Atmosphere - Tables and Data to 300 Standard Geopotential Kilometers*. Geophys. Res. Dir. and U.S. Weather Bureau, 1958.
5. Lina, Lindsay J., and Maglieri, Domenic J.: *Ground Measurements of Airplane Shock-Wave Noise at Mach Numbers to 2.0 and at Altitudes to 60,000 Feet*. NASA TN D-235, 1960.
6. Maglieri, Domenic J., Hubbard, Harvey H., and Lansing, Donald L.: *Ground Measurements of the Shock-Wave Noise From Airplanes in Level Flight at Mach Numbers to 1.4 and at Altitudes to 45,000 Feet*. NASA TN D-48, 1959.
7. Maglieri, Domenic J., Huckel, Vera, and Parrott, Tony L.: *Ground Measurements of Shock-Wave Pressure for Fighter Airplanes Flying at Very Low Altitudes and Comments on Associated Response Phenomena*. NASA TM X-611, 1961.
8. Lansing, Donald L.: *Some Effects of Flight Path Upon the Distribution of Sonic Booms*. *Proc. Symposium on Atmospheric Acoustic Propagation*, vol. I, June 14-16, 1961, pp. 24-43. (Sponsored by U.S. Army Signal Missile Support Agency and Texas Western College.)
9. Whitham, G. B.: *The Behavior of Supersonic Flow Past a Body of Revolution, Far From the Axis*. *Proc. Roy. Soc. (London)*, ser. A, vol. 201, no. 1064, Mar. 7, 1950, pp. 89-109.
10. Carlson, Harry W.: *An Investigation of the Influence of Lift on Sonic-Boom Intensity by Means of Wind-Tunnel Measurements of the Pressure Fields of Several Wing-Body Combinations at a Mach Number of 2.01*. NASA TN D-881, 1961.
11. Maglieri D. J., Parrott, T. L., Hilton, D. A., and Copeland, W. L.: *Lateral-Spread Sonic-Boom Ground-Pressure Measurements From Airplanes at Altitudes to 75,000 Feet and at Mach Numbers to 2.0*. NASA TN D-2021, 1963.

12. Carlson, Harry W.: Wind-Tunnel Measurements of the Sonic-Boom Characteristics of a Supersonic Bomber Model and a Correlation With Flight-Test Ground Measurements. NASA TM X-700, 1962.
13. Randall, D. G.: Methods for Estimating Distributions and Intensities of Sonic Bangs. R. & M. No. 3113, British A.R.C., 1959.
14. Walkden, F.: The Shock Pattern of a Wing-Body Combination, Far From the Flight Path. Aero. Quarterly, vol. IX, pt. 2, May 1958, pp. 164-194.

BIBLIOGRAPHY

- DuMond, Jesse W. M., Cohen, E. Richard, Panofsky, W. K. H., and Deeds, Edward: A Determination of the Wave Forms and Laws of Propagation and Dissipation of Ballistic Shock Waves. Jour. Acous. Soc. of America, vol. 18, no. 1, July 1946, pp. 97-118.
- Whitham, G. B.: The Behavior of Supersonic Flow Past a Body of Revolution, Far From the Axis. Proc. Roy. Soc. (London), ser. A, vol. 201, no. 1064, Mar. 7, 1950, pp. 89-109.
- Warren, C. H. E.: Sonic Bangs, A Qualitative Explanation. Tech. Notes Aero. 2192 and 2192a, British R.A.E., Sept. 1952.
- Whitham, G. B.: The Flow Pattern of a Supersonic Projectile. Communications on Pure and Appl. Math., vol. V, no. 3, Aug. 1952, pp. 301-348.
- Lilley, G. M., Westley, R., Yates, A. H., and Busing, J. R.: On Some Aspects of the Noise Propagation From Supersonic Aircraft. Rep. No. 71, The College of Aeronautics, Cranfield (British), Feb. 1953.
- Warren, C. H. E.: An Estimation of the Occurrence and Intensity of Sonic Bangs. Tech. Note Aero. 2334, British R.A.E., 1954.
- Daum, Fred L., and Smith, Norman: Experimental Investigation of the Shock Wave Pressure Characteristics Related to the Sonic Boom. WADC-TN-55-203, U.S. Air Force, Aug. 1955.
- Busemann, Adolf: The Relation Between Minimizing Drag and Noise at Supersonic Speeds. Proc. Conf. on High-Speed Aeronautics, Antonio Ferri, Nicholas J. Huff, and Paul A. Libby, eds., Polytechnic Inst. of Brooklyn, c.1955, pp. 133-144.
- Rao, P. Sambasiva: Supersonic Bangs - Part 1. Aero. Quarterly, vol. VII, pt. I, Feb. 1956, pp. 21-44.
- Rao, P. Sambasiva: Supersonic Bangs - Part 2. Aero. Quarterly, vol. VII, pt. II, May 1956, pp. 135-155.
- Mullens, Marshall E.: A Flight Test Investigation of the Sonic Boom. AFFTC-TN-56-20, Air Res. and Dev. Command, U.S. Air Force, May 1956.
- Whitham, G. B.: On the Propagation of Weak Shock Waves. Jour. Fluid Mech., vol. I, pt. 3, Sept. 1956, pp. 290-318.
- Whitham, G. B.: A New Approach to the Problems of Shock Dynamics - Part 1. Two Dimensional Problems. Jour. Fluid Mech., vol. 2, pt. 2, Mar. 1957, pp. 145-171.

- Struble, R. A., Stewart, C. E., Brown, E. A., and Ritter, A.: Theoretical Investigations of Sonic Boom Phenomena. WADC Tech. Rep. 57-412 (ASTIA Doc. No. AD 130883), U.S. Air Force, Aug. 1957.
- Jordan, Gareth H., Keener, Earl R., and Butchart, Stanley P.: Airplane Motions and Loads Induced by Flying Through the Flow Field Generated by an Airplane at Low Supersonic Speeds. NACA RM H57D17a, 1957.
- Walkden, F.: The Shock Pattern of a Wing-Body Combination, Far From the Flight Path. Aero. Quarterly, vol. IX, pt. 2, May 1958, pp. 164-194.
- Holbeche, T. A.: A Preliminary Data Report on Ground Pressure Disturbances Produced by the Fairey Delta 2 in Level Supersonic Flight. R & M No. 3296, British ARC., June 1958.
- Freeman, N. C., and Lam, S. H.: A Note on the Pressure Disturbance at Ground Level Caused by High-Flying Supersonic Aircraft. Rep. No. 444 (AFOSR TN-58-1127 AD 207 781), Princeton Univ., Dec. 1958.
- Whitham, G. B.: A New Approach to Problems of Shock Dynamics - Part 2. Three-Dimensional Problems. Jour. Fluid Mech., vol. 5, pt. 3, Apr. 1959, pp. 369-386.
- Maglieri, Domenic J., and Carlson, Harry W.: The Shock-Wave Noise Problem of Supersonic Aircraft in Steady Flight. NASA MEMO 3-4-59L, 1959.
- Arde Associates: Response of Structures to Aircraft Generated Shock Waves. WADC Tech. Rep. 58-169, U.S. Air Force, Apr. 1959.
- Kerr, T. H.: Experience of Supersonic Flying Over Land in the United Kingdom. Rep. 250, AGARD, North Atlantic Treaty Organization (Paris), Sept. 1959.
- Maglieri, Domenic J., Hubbard, Harvey H., and Lansing, Donald L.: Ground Measurements of the Shock-Wave Noise From Airplanes in Level Flight at Mach Numbers to 1.4 and at Altitudes to 45,000 Feet. NASA TN D-48, 1959.
- Jordan, Gareth H.: Some Aspects of Shock Wave Generation by Supersonic Airplanes. Rep. 251, AGARD, North Atlantic Treaty Organization (Paris), Sept. 1959.
- Carlson, Harry W.: An Investigation of Some Aspects of the Sonic Boom by Means of Wind-Tunnel Measurements of Pressures About Several Bodies at a Mach Number of 2.01. NASA TN D-161, 1959.
- Randall, D. G.: Methods for Estimating Distributions and Intensities of Sonic Bangs. R. & M. No. 3113, British A.R.C., 1959.
- Lina, Lindsay J., Maglieri, Domenic J., and Hubbard, Harvey H.: Supersonic Transports - Noise Aspects With Emphasis on Sonic Boom. 2nd Supersonic Transports (Proceedings). S.M.F. Fund Paper No. FF-26, Inst. Aero. Sci., Jan. 25-27, 1960, pp. 2-12.

- Lina, Lindsay J., and Maglieri, Domenic J.: Ground Measurements of Airplane Shock-Wave Noise at Mach Numbers to 2.0 and at Altitudes to 60,000 Feet. NASA TN D-235, 1960.
- Lilley, G. M., and Spillman, J. J.: Ground Level Disturbance From Large Aircraft Flying at Supersonic Speeds. CoA Note No. 103, College of Aeronautics, Cranfield (British), May 1960.
- Anon.: Lifting Effects in Sonic Boom. Rep. D6-5845, Boeing Airplane Co., Sept. 30, 1960.
- Morris, John: An Investigation of Lifting Effects on the Intensity of Sonic Booms. Jour. R.A.S., vol. 64, no. 598, Oct. 1960, pp. 610-616.
- Smith, Harriet J.: Experimental and Calculated Flow Fields Produced by Airplanes Flying at Supersonic Speeds. NASA TN D-621, 1960.
- Lansing, Donald L.: Calculated Effects of Body Shape on the Bow Shock Overpressures in the Far Field of Bodies in Supersonic Flow. NASA TR R-76, 1960.
- Ryhming, I. L.: The Supersonic Boom of a Projectile Related to Drag and Volume. Jour. Aerospace Sci., vol. 28, no. 2, Feb. 1961, pp. 113-118, 157.
- Ryhming, I. L., and Yoler, Y. A.: Supersonic Boom of Wing-Body Configurations. Jour. Aerospace Sci., vol. 28, no. 4, Apr. 1961, pp. 313-320.
- Power, J. Kenneth: Some Considerations of Sonic Boom. FAA, May 1961.
- Jones, L. B.: Lower Bounds for Sonic Bangs. Jour. R.A.S. (Tech. Notes), vol. 65, no. 606, June 1961, pp. 433-436.
- Lansing, Donald L.: Some Effects of Flight Path Upon the Distribution of Sonic Booms. Proc. Symposium on Atmospheric Acoustic Propagation, vol. 1, June 14-16, 1961, pp. 24-43. (Sponsored by U.S. Army Signal Missile Support Agency and Texas Western College.)
- Maglieri, Domenic J., and Hubbard, Harvey H.: Ground Measurements of the Shock-Wave Noise From Supersonic Bomber Airplanes in the Altitude Range From 30,000 to 50,000 Feet. NASA TN D-880, 1961.
- Jordan, Gareth H., McLeod, Norman J., and Ryan, Bertha M.: Review of Flight Measurements of Sonic Booms and Effects of Shock Waves on Other Aircraft. Presented at Soc. of Exp. Test Pilots 5th Annual Symposium (Beverly Hills, Calif.), Sept. 29-30, 1961.
- Warren, C. H. E.: A Preliminary Analysis of the Results of Exercise Crackerjack, and Their Relevance to Supersonic Transport Aircraft. Tech. Note No. Aero2789, British R.A.E., Sept. 1961.

- Maglieri, Domenic J., Huckel, Vera, and Parrott, Tony L.: Ground Measurements of Shock-Wave Pressures for Fighter Airplanes Flying at Very Low Altitudes and Comments on Associated Response Phenomena. NASA TM X-611, 1961.
- Kane, E. J.: Determination of the Far Field From Ballistic Range Sonic Boom Test Data. Doc. No. D6-7165, Boeing Airplane Co., Feb. 1961.
- Sigalla, A., and Kane, E. J.: A Proposal For the Investigation of the Factors Which Affect Sonic Boom Intensity. Doc. No. D6-7357, Apr. 1961.
- Sigalla, A.: Note on Some Theoretical Aspects of Lift Produced Sonic Boom. Doc. No. D6-7996, Boeing Airplane Co., 1961.
- Carlson, Harry W.: An Investigation of the Influence of Lift on Sonic-Boom Intensity by Means of Wind-Tunnel Measurements of the Pressure Fields of Several Wing-Body Combinations at a Mach Number of 2.01. NASA TN D-881, 1961.
- Parrott, T. L.: Experimental Studies of Glass Breakage Due to Sonic Booms. Sound, vol. 1, no. 3, May-June 1962, pp. 18-21.
- Reed, Jack W.: Atmospheric Focusing of Sonic Boom. Jour. Appl. Meteorology, vol. 1, no. 2, June 1962, pp. 265-267.
- Carlson, Harry W.: The Lower Bound of Attainable Sonic-Boom Overpressure and Design Methods of Approaching This Limit. NASA TN D-1494, 1962.
- Carlson, Harry W.: Wind-Tunnel Measurements of the Sonic-Boom Characteristics of a Supersonic Bomber Model and a Correlation With Flight-Test Ground Measurements. NASA TM X-700, 1962.
- Kane, E. J.: Sonic Boom - State of the Art (1961). Doc. No. D6-8965, Boeing Airplane Co., May 1962.
- Clarke, M. J., and Wilby, J. F.: Subjective Response to Sonic Bangs. C.P. No. 588, British A.R.C., 1962.
- Morris, Odell A.: A Wind-Tunnel Investigation at a Mach Number of 2.01 of the Sonic-Boom Characteristics of Three Wing-Body Combinations Differing in Wing Longitudinal Location. NASA TN D-1384, 1962.
- Maglieri, Domenic J., and Lansing, Donald L.: Sonic Booms From Aircraft in Maneuvers. Sound, vol. 2, no. 2, Mar.-Apr. 1963, pp. 39-42.
- Power, J. K., and Bates, George: Sonic Boom & Community Relations. [Preprint] 683B, Soc. Automotive Eng., Apr. 1963.
- Warren, C. H. E.: The Effect of Meteorological Variations on the Statistical Spread in the Intensity of Bangs at Large Distances From the Source. Tech. Note Structures 334, British R.A.E., May 1963.

Maglieri, Domenic J., and Morris, Garland J.: Measurements of the Response of Two Light Airplanes to Sonic Booms. NASA TN D-1941, 1963.

Friedman, Manfred P., Kane, Edward J., and Sigalla, Armand: Effects of Atmosphere and Aircraft Motion on the Location and Intensity of a Sonic Boom. AIAA Jour., vol. 1, no. 6, June 1963, pp. 1327-1335.

Maglieri, Domenic J., and Parrott, Tony L.: Atmospheric Effects on Sonic-Boom Pressure Signatures. Sound, vol. 2, no. 4, July-Aug. 1963, pp. 11-14.

Maglieri, Domenic J., Ritchie, Virgil S., and Bryant, John F., Jr.: In-Flight Shock-Wave Pressure Measurements Above and Below a Bomber Aircraft at Mach Numbers 1.42 to 1.69. NASA TN D-1968, 1963.

Carlson, Harry W.: The Influence of Airplane Configuration on Sonic-Boom Characteristics. Paper Presented at AIAA-ASD Vehicle Design and Propulsion Meeting (Dayton, Ohio), Nov. 1963.

Cawthorn, Jimmy M.: Some Sonic-Boom Induced Building Responses. Paper Presented at Sixty-Sixth Meeting of Acoustical Soc. of America (Ann Arbor, Mich.), Nov. 1963.

Maglieri, D. J., Parrott, T. L., Hilton, D. A., and Copeland, W. L.: Lateral-Spread Sonic-Boom Ground-Pressure Measurements From Airplanes at Altitudes to 75,000 Feet and at Mach Numbers to 2.0. NASA TN D-2021, 1963.

Carlson, Harry W., and Morris, Odell A.: Wind-Tunnel Investigation of the Sonic-Boom Characteristics of a Large Supersonic Bomber Configuration. NASA TM X-898, 1963.

Barger, Raymond L.: Some Effects of Flight Path and Atmospheric Variations on the Boom Propagated From a Supersonic Aircraft. NASA TR R-191, 1964.

TABLE I.- SONIC-BOOM TEST FLIGHTS

Flight test	Date	Time of day	Airplane				Type of flight	Purpose of flight		
			Type	Weight, lb	Altitude, ft	Mach number		Atmospheric effect	Superboom	Generation and propagation
1	9- 1-61	1345	Fighter		41.2 x 10 ³	1.52	Steady			x
2	9- 6-61	1245	Fighter		40.5	1.37	Steady			x
3	9- 6-61	1253	Fighter		42.0	1.45	Steady			x
4	9-11-61	1000	Fighter		53.1	1.92	Steady	x		
5	9-11-61	1400	Fighter		51.0	1.92	Steady	x		
6	9-13-61	0940	Fighter		51.0	1.93	Steady	x		
7	9-14-61	0800	Fighter		40 to 20	1.2 to 1.5	Maneuver		x	
8	9-14-61	0810	Fighter		40 to 20	1.2 to 1.5	Maneuver		x	
9	9-14-61	0820	Fighter		40 to 20	1.2 to 1.5	Maneuver		x	
10	9-15-61	1235	Fighter		40 to 20	.9 to 1.4	Maneuver		x	
11	9-15-61	1242	Fighter		40 to 20	.9 to 1.4	Maneuver		x	
12	9-15-61	1248	Fighter		40 to 20	.9 to 1.4	Maneuver		x	
13	9-15-61	1254	Fighter		40 to 20	.9 to 1.4	Maneuver		x	
14	9-18-61	0834	Fighter		10.3	1.24	Steady			x
15	9-18-61	0840	Fighter		14.6	.9 to 1.16	Maneuver		x	
16	9-18-61	0846	Fighter		14.2	.9 to 1.17	Maneuver		x	
17	9-21-61	0820	Fighter		32.2	1.48	Maneuver		x	
18	9-21-61	0828	Fighter		32.2	1.43	Maneuver		x	
19	9-21-61	0835	Fighter		32.2	1.42	Maneuver		x	
20	9-22-61	0933	Fighter		14.2	.9 to 1.17	Maneuver		x	
21	9-22-61	0942	Fighter		33.3	1.52	Maneuver		x	
22	9-22-61	0953	Fighter		43.2	1.44	Steady			x
23	9-25-61	0855	Fighter		14.0	.9 to 1.11	Maneuver		x	
24	9-25-61		Fighter		(a)	(a)	Maneuver			
25	9-25-61	0912	Fighter		32.2	1.34	Steady			x
26	9-28-61	0850	Bomber	76,980	(b)	(b)	Steady			
27	9-28-61	0900	Bomber	70,980	61.5	1.95	Steady			x
28	9-28-61	0910	Bomber	65,930	62.4	1.96	Steady			x
29	9-29-61	1430	Fighter		33.6	1.13	Steady			x
30	9-29-61	1435	Fighter		32.8	1.69	Steady			x
31	10- 2-61	0910	Bomber	82,280	62.1	2.0	Steady			x
32	10- 3-61	0905	Fighter		33.7	1.5	Maneuver		x	
33	10- 3-61	0908	Fighter		33.7	1.5	Maneuver		x	
34	10- 4-61	0845	Bomber	84,980	61.1	2.0	Steady			x
35	10- 4-61	0855	Bomber	74,780	63.0	2.0	Steady			x
36	10- 4-61	0907	Bomber	66,780	65.3	2.0	Steady			x
37	10- 5-61	0938	Fighter		40 to 20	1.2 to 1.5	Maneuver		x	
38	10- 5-61	0946	Fighter		40 to 20	1.2 to 1.5	Maneuver		x	
39	10- 5-61	0954	Fighter		40 to 20	1.2 to 1.5	Maneuver		x	
40	10- 6-61	1005	Bomber	83,800	61.5	2.0	Steady			x
41	10- 6-61	1012	Bomber	78,800	64.0	1.98	Steady			x
42	10- 6-61	1022	Bomber	70,800	65.6	1.97	Steady			x
43	10- 6-61	1031	Bomber	64,000	61.3	2.0	Steady			x
44	10- 9-61	0841	Fighter		33.7	1.41	Steady			x
45	10- 9-61		Fighter		(c)	(c)	(c)			
46	10-10-61	0842	Bomber	85,200	51.6	2.0	Steady	x		x
47	10-10-61	0850	Bomber	74,800	49.7	1.96	Steady	x		x
48	10-10-61	0901	Bomber	67,700	70.7	1.72	Steady			x
49	10-10-61	0906	Bomber	64,000	59.5	2.0	Steady			x
50	10-10-61	1025	Fighter		51.1	1.4	Steady			x
51	10-12-61	0815	Bomber	89,200	42.1	1.80	Steady	x		x
52	10-12-61	0822	Bomber	79,900	41.2	1.85	Steady	x		x
53	10-12-61	0830	Bomber	70,400	31.2	1.5	Steady	x		x
54	10-12-61	0836	Bomber	63,600	31.2	1.5	Steady	x		x
55	10-12-61	1420	Fighter		21.7	1.35	Steady	x		
56	10-12-61	1426	Fighter		22.0	1.23	Steady	x		
57	10-12-61	1432	Fighter		21.8	1.11	Steady	x		
58	10-13-61	0948	Fighter		14.0	.9 to 1.22	Maneuver		x	
59	10-13-61	0954	Fighter		14.0	.9 to 1.24	Maneuver		x	
60	10-13-61	1000	Fighter		13.8	.9 to 1.22	Maneuver		x	
61	10-17-61	0900	Bomber	83,200	72.0	1.60	Steady			x
62	10-17-61	0915	Bomber	71,200	74.7	1.65	Steady			x
63	10-17-61	0920	Bomber	65,200	50.0	2.0	Steady			x

^aNo data - tracking failure.

^bNo data - instrument failure.

^cNo data - communications failure.